Journal of Medicinal Chemistry

Article

Discovery of N-((1-(4-(3-(3-((6,7-dimethoxyquinolin-3-yl)oxy)phenyl)ureido)-2-(trifluoromethyl)phenyl)piperidin-4-yl)methyl)propionamide (CHMFL-KIT-8140) as a Highly Potent Type II Inhibitor Capable of Inhibiting the T670I "Gatekeeper" Mutant of cKIT Kinase

Binhua Li, Aoli Wang, Juan Liu, Ziping Qi, Xiaochuan Liu, Kailin Yu, Hong Wu, Cheng Chen, Chen Hu, Wenchao Wang, Jiaxin Wu, Zhenquan Hu, Ling Ye, Fengming Zou, Feiyang Liu, Beilei Wang, Li Wang, Tao Ren, Shaojuan Zhang, Mingfeng Bai, Shanchun Zhang, Jing Liu, and Qingsong Liu

J. Med. Chem., **Just Accepted Manuscript** • DOI: 10.1021/acs.jmedchem.6b00902 • Publication Date (Web): 22 Aug 2016

Discovery of *N*-((1-(4-(3-(3-((6,7-dimethoxyquinolin-3-yl)oxy)phenyl)ureido)-2-(trifluoromethyl)phenyl)piperidin-4-yl)methyl)propionamide (CHMFL-KIT-8140) as a Highly Potent Type II Inhibitor Capable of Inhibiting the T670I "Gatekeeper" Mutant of cKIT Kinase

Binhua Li[1,2,7], Aoli Wang[1,3,7], Juan Liu[1,7], Ziping Qi[1,2,7], Xiaochuan Liu[1,7], Kailin Yu[1,3], Hong Wu[1], Cheng Chen[1,2], Chen Hu[1,3], Wenchao Wang[1,2], Jiaxin Wu[1,3], Zhenquan Hu[1,2], Ling Ye[4], Fengming Zou[1,2], Feiyang Liu[1,3], Beilei Wang[1,2], Li Wang[1,2], Tao Ren[4], Shaojuan Zhang[5], Mingfeng Bai[5], Shanchun Zhang[2,6], Jing Liu[1,2], Qingsong Liu[1,2,3,4*]*

1. High Magnetic Field Laboratory, Chinese Academy of Sciences, Mailbox 1110, 350 Shushanhu Road, Hefei, Anhui 230031, P. R. China
2. CHMFL-HCMTC Target Therapy Joint Laboratory, 350 Shushanhu Road, Hefei Anhui 230031, P. R. China
3. University of Science and Technology of China, Hefei, Anhui 230036, P. R. China

4. Precision Targeted Therapy Discovery Center, Institute of Technology Innovation, Hefei Institutes of Physical Science, Chinese Academy of Sciences, Hefei, Anhui 230088, P. R. China

5. Molecular Imaging Laboratory, Department of Radiology, University of Pittsburgh, Pittsburgh, PA 15219, USA; Department of Bioengineering, University of Pittsburgh, Pittsburgh, PA 15261, USA; University of Pittsburgh Cancer Institute, Pittsburgh, PA 15232, USA.

6. Hefei Cosource Medicine Technology Co. LTD., 358 Ganquan Road, Hefei, Anhui 230031, P. R. China

7. These authors contribute equally

ABSTRACT

cKIT kinase inhibitors, *e.g.* Imatinib could induce drug-acquired mutations such as cKIT T670I that rendered drug resistance after chronic treatment. Through a type II kinase inhibitor design approach we discovered a highly potent type II cKIT kinase inhibitor compound **35** (CHMFL-KIT-8140), which potently inhibited both cKIT wt (IC_{50}: 33 nM) and cKIT gatekeeper T670I mutant (IC_{50}: 99 nM). Compound **35** displayed strong anti-proliferative effect against GISTs cancer cell lines GIST-T1 (cKIT wt, GI_{50}: 4 nM) and GIST-5R (cKIT T670I, GI_{50}: 26 nM). In the cellular context it strongly inhibited c-KIT mediated signaling pathways and induced apoptosis. In the BaF3-TEL-cKIT-T670I isogenic cell inoculated xenograft mouse model, **35** exhibited dose dependent tumor growth suppression efficacy and 100 mg/kg dosage provided 47.7% tumor growth inhibition (TGI) without obvious toxicity. We believe compound **35** would be a good pharmacological tool for exploration of the cKIT-T670I mutant mediated pathology in GISTs.

INTRODUCTION

Gastrointestinal stromal tumors (GISTs) are the most common mesenchymal tumors of the gastrointestinal tract. There are approximately 1-2/100,000 newly diagnosed patients with GISTs each year in the US.[1] Almost all GISTs express cKIT kinase and about 80–85% of all GISTs cases are associated with gain-of-function mutations in the cKIT gene.[2] c-KIT kinase is a member of the type III transmembrane receptor tyrosine kinase (RTK) family. Under physiological conditions, it gets activated upon binding of the extracellular stem cell factor (SCF). cKIT plays important roles in cellular transformation and differentiation, including proliferation, survival, adhesion, and chemotaxis.[3] Constitutive activation of the cKIT kinase is critical in the pathogenesis of GISTs.[4,5] Due to the critical role of cKIT kinase to the tumorigenesis of GISTs, it has been extensively explored as an important drug discovery target for anti-GIST therapy.

Currently there are two cKIT kinase inhibitors approved for the clinical use for GISTs. Compound **1** (Imatinib[6], Figure 1) was the first type II kinase inhibitor approved as the first-line treatment for advanced GIST. Unfortunately, approximately 14% of patients are initially insensitive to compound **1**,[7,8] furthermore, 46% to 67% of the responding patients will develop resistance through acquisition of a secondary mutation in the cKIT kinase domain,[9-11] *e.g.* the ATP-binding pocket mutants V654A and T670I, within 2 years of compound **1** treatment**.** The T670 residue located at the gatekeeper position in cKIT kinase provides one of the key hydrogen bonds for the binding of **1**. Therefore, mutations at this position have a profound effect for compound **1**'s binding.[12] In addition, experimental evidence supports that cKIT T670I mutant will drive a more aggressive earlier metastasis and shorter progression-free survival.[13] Compound **2** **(**Sunitinib), a type I kinase inhibitor, was approved by FDA for the treatment of patients with Imatinib-resistant GIST in 2006. Because compound **2** does not occupy the deep

hydrophobic pocket generated by DFG motif flip-out as type II inhibitor compound **1** does, there is enough space to accommodate the more bulky amino acid residue Isoleucine associated with the T670I mutation without affecting **2**'s binding.[12] Moreover, a panel of small molecule type II kinase inhibitors have been reported to bear cKIT kinase inhibitory activity such as **3** (Nilotinib),[14] **4** (Masitinib),[15] **5** (Sorafenib),[16] etc. Among them compound **3** and **4** significantly lost activity against T670I mutant, while compound **5** exhibited moderate inhibitory activity. Here, we reported our medicinal chemistry effort that started from a hit compound **6** to the discovery of a new quinoline scaffold based type II cKIT kinase inhibitor compound **35** (CHMFL-KIT-8140), which displayed potent in vitro and in vivo activities against cKIT gatekeeper T670I mutant (Figure 2).

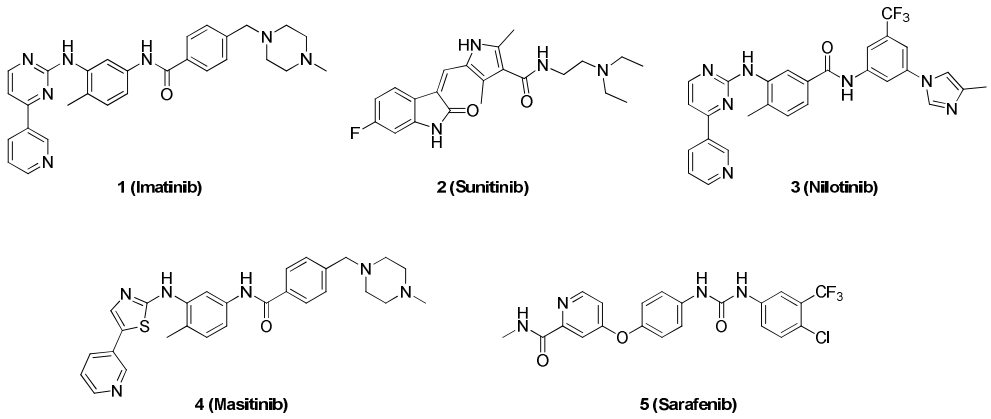

Figure 1. Chemical structures of the representative cKIT kinase inhibitors.

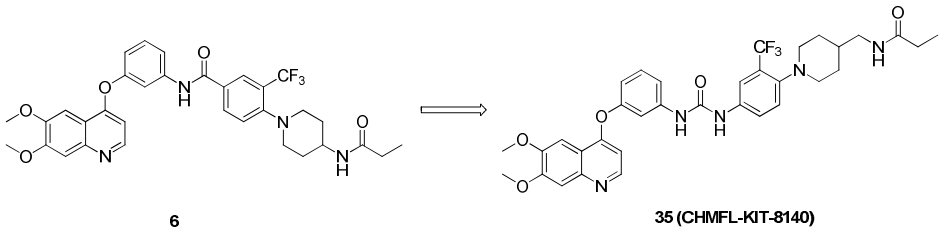

Figure 2. Schematic illustration of discovery of compound **35** (CHMFL-KIT-8140).

RESULTS AND DISCUSSION

Structure-Activity Relation (SAR) Exploration

During high-throughput screening of our in-house generated kinase inhibitors, we obtained a quinoline scaffold based compound **6** which exhibited moderate anti-proliferative activity against BaF3-TEL-cKIT cell line (GI_{50}: 0.4 μM) and BaF3-TEL-cKIT-T670I cell line (GI_{50}: 2.7 μM). However, the compound demonstrated a good selectivity window against the parental BaF3 cell line (GI_{50}: >10 μM). Therefore, we decided to use **6** as the starting point for further medicinal chemistry modification. In order to get a view of the structural basis for the SAR exploration, we first made a homology model of cKIT T670I mutant based on the cKIT wt X-ray crystal structure (PDB ID: 1T46) and examined the detailed binding information of compounds **1** and **6** with cKIT wt/T670I (Figure 3). In the cKIT wt, compound **1** forms four key hydrogen bonds: one in the hinge binding area between the pyridine nitrogen of **1** and Cys673; one in the linker moiety between the aminopyrimidine nitrogen of **1** and the gatekeeper residue Thr670; two canonical hydrogen bonds between the Glu640 in the c-Helix and Asp810 in the DFG motif with the amide bond of **1** (Figure 3A). The mutation of gatekeeper residue Thr670 to the more bulky Ile670 results in loss of one of the key hydrogen bonds and meanwhile the newly generated steric hindrance impeded compound **1**'s binding (Figure 3B). In comparison, in our model compound **6** forms three key hydrogen bonds with cKIT wt, *i.e.* one in the hinge binding area and two in the DFG motif and c-Helix area (Figure 3C). Compound **6** has an *O*-linked phenyl ring in the gatekeeper area and lacks the hydrogen bond formed between Thr670 with compound **1**. However, the *O*-linked phenyl ring in **6** will be likely to generate enough space to accommodate the more bulky Ile670 if it can orientate into a proper direction, which will make it possible to overcome the T670I mutation (Figure 3D). In addition, the CF3 group in **6** might form

hydrophobic interactions with Leu647, Ile653, Leu783 and Ile808 in cKIT, which could be beneficial to the binding (Figure 3E). Based on the analysis and the typical type II kinase inhibitor design approach,[17] compound **6** was divided into four parts: the quinoline hinge binding part, the *O*-bridged phenyl linker part, the amide mediated hydrogen bonding part and the tail part that occupies the DFG shifting created hydrophobic pocket (Figure 3F). Since the quinoline occupied hinge binding part is required for binding and the *O*-bridged phenyl linker part is necessary for overcoming cKIT-T670I mutation, we decided to keep them unchanged. We envisioned that variation of the H-bonding area (**R1**) and the tail part (**R2**, **R3**) might alter the orientation of the *O*-bridged phenyl linker moiety to achieve higher binding affinity and better selectivity against cKIT-T670I kinase mutant.

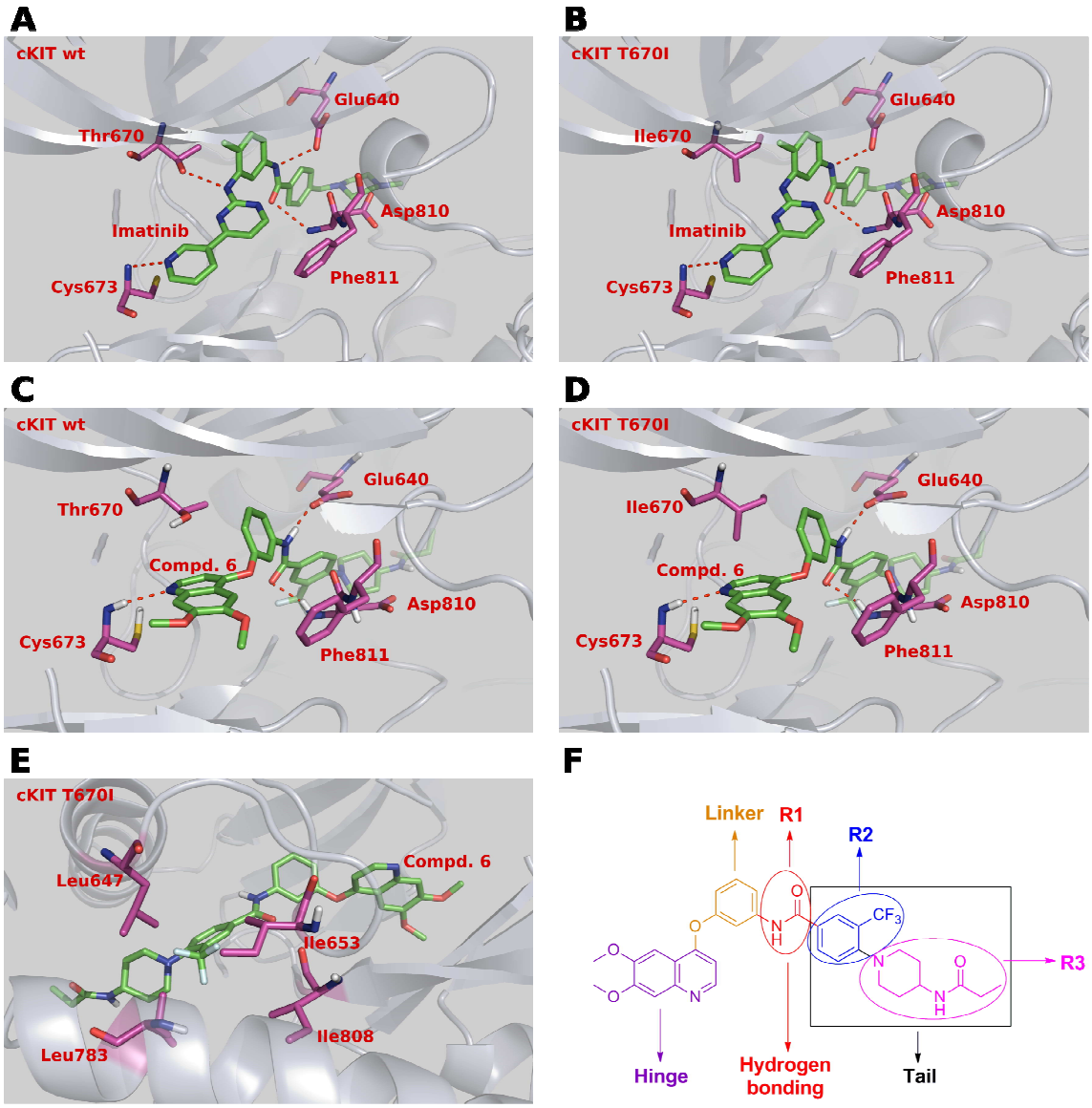

Figure 3. Schematic illustration of SAR exploration rationale. (A) Binding mode of compound **1** with cKIT wt (PDB ID: 1T46). (B) Binding mode of compound **1** with cKIT T670I homology model (generated based on PDB ID: 1T46). (C) Binding mode of compound **6** with cKIT wt (PDB ID: 1T46, docking model). (D) Binding mode of compound **6** with cKIT T670I homology model (generated based on PDB ID: 1T46, docking model). (E) Illustration of the hydrophobic interaction between the CF3 group of compound **6** and Leu647, Ile653, Leu783 and Ile808. (F) Illustration of the chemical modification strategy of compound **6**.

As the starting point, we first explored the SAR of the hydrogen bonding part (**R1**). BaF3-TEL-cKIT, BaF3-TEL-cKIT-T670I and parental BaF3 cells were used to monitor the cKIT wt

and cKIT-T670I kinase inhibitory activities. Replacement of the amide group in compound **6** with urea group (**7**) significantly increased the activity both to cKIT wt (GI_{50}: 0.12 μM) and cKIT T670I (GI_{50}: 0.071 μM), meanwhile showed a selectivity ratio of approximately 12 against parental BaF3 cells (GI_{50}: 1.5 μM) (Table 1). However, switching the amide group to a much larger group, *i.e.*, *N,N'*-dimethylcyclopropane-1,1-dicarboxamide (**8**), led to the complete loss of activity to both the c-KIT wt and cKIT-T670I (GI_{50}: >10 μM). This might be due to the interaction of the cyclopropane substituent with the Glu640, which abolished the critical hydrogen bonds in this area for the type II binding. We then explored the **R2** moiety in the tail part by fixing the **R1** as the uera. Removal of the trifluoromethyl group (**9**) also caused complete activity loss to cKIT wt and cKIT-T670I (GI_{50}: >10 μM), which indicated that the hydrophobic interaction between the CF3 group and the hydrophobic environment formed by Leu647, Ile653 Leu783 and Ile808 was important for the binding. In addition, replacement of the phenyl group with a pyridine group (**10**) resulted in significant activity loss in BaF3-TEL-cKIT-T670I cells (GI_{50}: ＞10 μM). These results indicated that the urea group at the **R1** position and the (trifluoromethyl)benzyl group at **R2** were preferred for better activity.

Table 1. SAR Exploration Focused on the **R1/R2** positons[a]

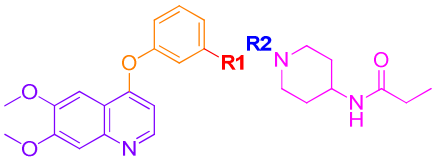

Compd	**R1**	**R2**	BaF3-TEL-cKIT (GI_{50}: μM)	BaF3-TEL-cKIT-T670I (GI_{50}: μM)	BaF3 (GI_{50}: μM)
6		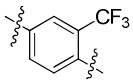	0.4±0.011	2.7±0.058	＞10

7	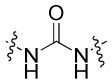	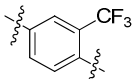	0.12±0.016	0.071±0.0011	1.5±0.17
8	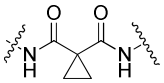	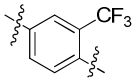	＞10	＞10	＞10
9	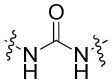	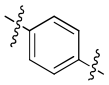	＞10	＞10	＞10
10	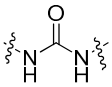	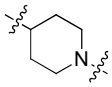	0.34±0.01	＞10	＞10

[a]All GI_{50} values were obtained by triplet testing.

On the basis of compound **7**, we next focused SAR exploration on the **R3** position, which presumably occupies the DFG-out shifting generated hydrophobic pocket and usually will provide the selectivity and higher binding affinity for the type II inhibitors (Table 2). Shifting the propionyl group from 4-position (**7**) to 3-position (**11**) led to about 13-fold activity loss in BaF3-TEL-cKIT-T670I cells (GI_{50}: 0.071μM versus 0.92 μM). Replacement of the propionyl group in **7** with acetyl group (**12**) retained the activities against BaF3-TEL-cKIT cells and BaF3-TEL-cKIT-T670I cells (GI_{50}: 0.11 μM and 0.046 μM, respectively), meanwhile displayed better selectivity against parental BaF3 cells (GI_{50}: 7.1 μM). Installment of larger groups such as dimethylbutyl (**13**), glycine (**14**) and alanine (**15**) all led to about 10-fold loss of activity against cKIT T670I mutant. However, the *N,N*-dimethylglycine (**16**) gained back the activity against cKIT T670I mutant (GI_{50}: 0.053 μM) and displayed better activity against cKIT wt (GI_{50}: 0.038 μM) as well as better selectivity to parental BaF3 cells (GI_{50}: 2.9 μM) compared to **7**. Introduction of cyclohexene (**17**) and pyridine groups (**18**) both led to about 5-10 fold activity loss, while tetrahydropyran group (**19**) gained back the activity against both cKIT wt (GI_{50}: 0.087

μM) and cKIT T670I (GI_{50}: 0.083 μM). *N*-Methyl piperidine (**20**) and *N*-ethyl piperidine (**21**) retained similar potency. *N*-Acyl (**22**), *N*-cyclopropanecarbonyl (**23**) and Boc (**24**) substituents caused 2-3 fold activity loss, and 2-methyl piperidine group (**25**) resulted in about 10-fold activity loss against cKIT T670I. Increasing the length or size of the piperidine-derived substituents either narrowed down the selectivity window to parental BaF3 cells (**26** and **27**) or decreased the activity against cKIT T670I (**28** and **29**). Interestingly, ethyl linked morpholine (**30**) showed impressive activities against cKIT wt (GI_{50}: 0.042 μM) and cKIT T670I (GI_{50}: 0.059 μM), meanwhile kept a good selectivity window to parental BaF3 cells (GI_{50}: 3.6 μM). Switching the amide moiety to sulfonamide derivatives with different aliphatic chains such as methyl (**31**), ethyl (**32**) and propyl (**33**) did not improve the anti-proliferative efficacy against cKIT T670I mutant either. However, introduction of the cyclopropyl group (**34**) started to gain back the activity against BaF3-TEL-cKIT-T670I cells (GI_{50}: 0.063 μM). Increasing the size of **R3** to *N*-(piperidin-4-ylmethyl)propionamide (**35**) enhanced the activity against cKIT wt (GI_{50}: 0.057 μM) meanwhile retained the activity against cKIT T670I and remarkably improved the selectivity window to parental BaF3 cells (GI_{50}: >10 μM). Unfortunately, further size increase (**36**) resulted in obvious activity loss compared to compound **35**.

Table 2. SAR Exploration Focused on the **R3** Position[a]

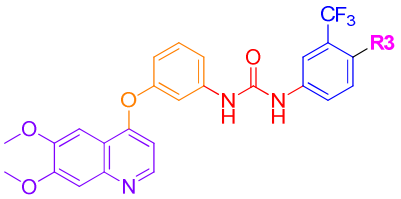

Compd	**R3**	BaF3-TEL-cKIT (GI_{50}: μM)	BaF3-TEL-cKIT-T670I (GI_{50}: μM)	BaF3 (GI_{50}: μM)

11	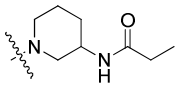	0.28±0.025	0.92±0.04	1.3±0.17
12	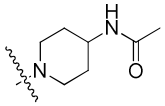	0.11±0.016	0.046±0.001	7.1±0.38
13	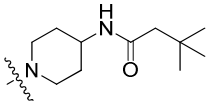	0.43±0.01	0.34±0.025	＞10
14	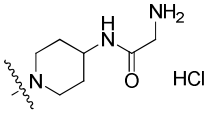	0.13±0.01	0.58±0.02	5±1.0
15	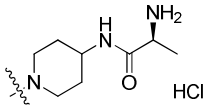	0.12±0.011	0.48±0.011	3±0.15
16	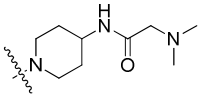	0.038±0.001	0.053±0.001	2.9±0.17
17	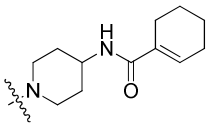	0.76±0.0057	0.76±0.1	1.1±0.47
18	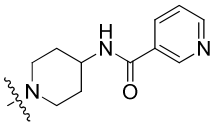	0.02±0.001	0.32±0.025	7±0.74
19	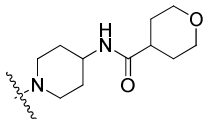	0.087±0.0015	0.083±0.021	2.9±0.056
20	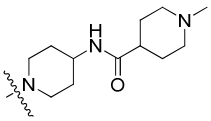	0.16±0.01	0.081±0.006	1.7±0.1
21	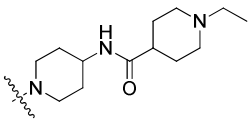	0.039±0.041	0.087±0.008	1.3±0.11
22	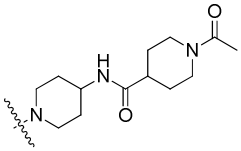	0.059±0.001	0.23±0.0001	3.4±1.2

23	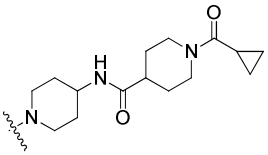	0.13±0.0057	0.12±0.02	0.8±0.084
24	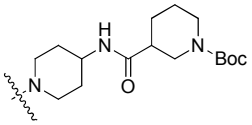	0.13±0.001	0.17±0.05	0.51±0.15
25	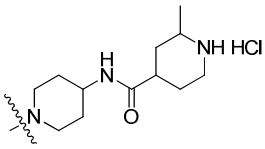	0.46±0.021	0.65±0.076	4.0±0.32
26	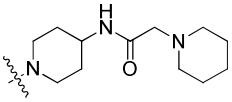	0.12±0.0001	0.037±0.009	0.48±0.006
27	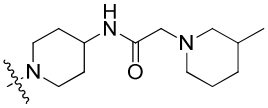	0.33±0.015	0.2±0.011	0.87±0.068
28	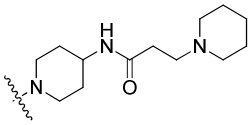	0.44±0.03	0.26±0.052	7.6±0.61
29	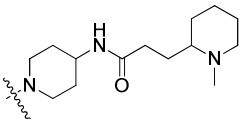	0.19±0.021	0.2±0.02	1.2±0.11
30	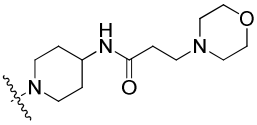	0.042±0.003	0.059±0.006	3.6±0.89
31	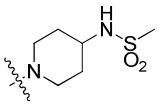	3.9±0.023	3.8±0.02	＞10
32	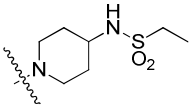	0.034±0.002	0.33±0.029	6.2±0.38
33	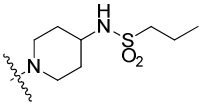	0.059±0.003	0.95±0.04	4.2±0.36
34	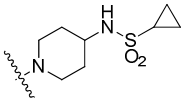	0.14±0.021	0.063±0.002	1.9±0.058

35	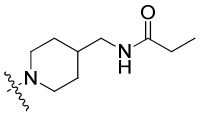	0.057±0.0021	0.063±0.001	＞10
36	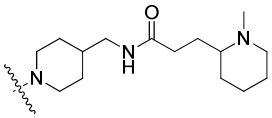	0.25±0.06	0.46±0.01	4.4±1.37

[a]All GI_{50} values were obtained by triplet testing.

Since compound **35** exhibited the best activity and selectivity profile, we then studied its binding modes with cKIT wt and T670I mutant by molecular modeling. In the cKIT wt (PDB ID: 1T46), compound **35** adopted a canonical type II binding mode. As expected, the quinoline nitrogen formed a hydrogen bond with the cKIT residue Cys673 in the hinge binding area (Figure 4A). The two NHs in the urea moiety formed two hydrogen bonds with Glu640 in the c-Helix, and the carbonyl formed a hydrogen bond with the Asp810 in the DFG motif. The tail part occupied the hydrophobic pocket generated by the DFG-out shift. In addition, a hydrogen bond was formed between the NH of the amide and the Ile789 in cKIT kinase. In the homology model of cKIT T670I mutant, compound **35** adopted the similar type II binding mode. The three hydrogen bonds formed via the urea moiety caused the *O*-bridged phenyl moiety in **35** to orient to an angle that provided enough space for the bulky residue Isoleucine, which could explain its potency against T670I mutant (Figure 4B).

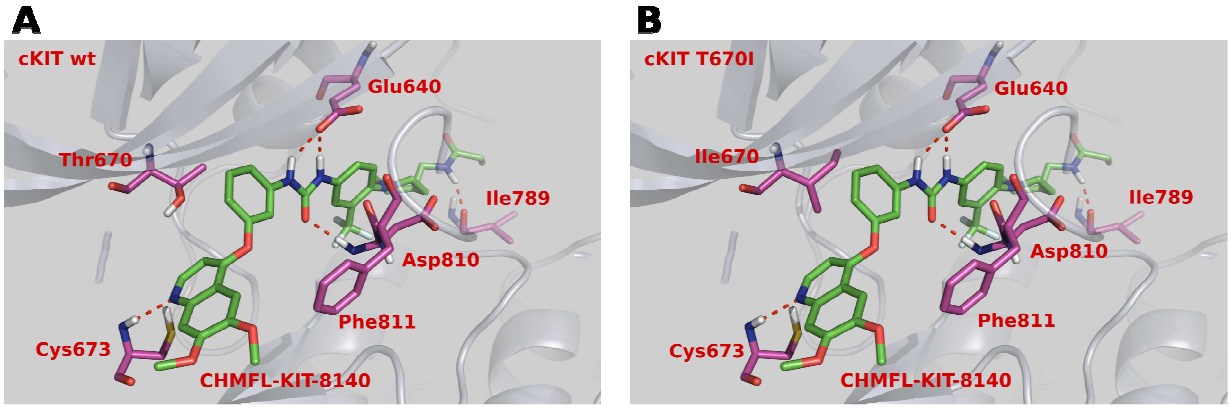

Figure 4. Molecular modeling analysis of the binding modes of cKIT wt/T670I with compound **35**. (A) Binding mode of compound **35** with cKIT wt (PDB ID: 1T46). (B) Binding mode of compound **35** with cKIT T670I homology model (generated based on PDB ID: 1T46).

Biochemical and Cellular Property Evaluation

We further examined the activity of compound **35** against a panel of cKIT mutants in the TEL engineered BaF3 systems as well as intact GIST cancer cell lines (Table 3). The results demonstrated that besides cKIT wt and cKIT T670I, compound **35** was also effective against cKIT L567P (GI_{50}: 0.023 μM), cKIT N822K (GI_{50}: 0.04 μM), and cKITT670I/V559D (GI_{50}: 0.073 μM). However, compound **1** was only potent against cKIT L567P (GI_{50}: 0.01 μM). Compound **2** was more potent against these mutants but it also affected the parental BaF3 cells growth (GI_{50}: 1.6 μM) which indicated its multiple target feature. In addition, compound **35** is about 10-fold and 2-fold more potent than compounds **1** and **2** against cKIT wt, respectively. Compound **35** displayed similar anti-proliferative effects to compound **2** against cKIT wt expressing GIST cancer cell line GIST-T1 (GI_{50}: 0.004 μM) and is about 7-fold more potent than compound **1** (GI_{50}: 0.027 μM). **35** also exhibited similar potency to compound **2** against cKIT T670I expressing GIST cancer cell line GIST-5R (GI_{50}: 0.026 μM) and was about 300-fold more active than compound **1** (GI_{50}: 8.3 μM).

Table 3. Anti-proliferative Effects of Compounds **1**, **2** and **35** against a Variety of BaF3-TEL-cKIT Isogenic Cells and GIST Intact Cell Lines[a]

Cell line	Compd. **1** GI_{50} (μM)	Compd. **2** GI_{50} (μM)	Compd. **35** GI_{50} (μM)
BaF3	＞10	1.6±0.15	＞10
BaF3-TEL-cKIT	0.59±0.050	0.11±0.040	0.057±0.002

BaF3-TEL-cKIT-T670I	9.6±0.32	0.005±0.0001	0.063±0.001
BaF3-TEL-cKIT-V654A	0.70±0.015	0.006±0.0003	0.32±0.040
BaF3-TEL-cKIT-L567P	0.01±0.001	0.003±0.0006	0.023±0.001
BaF3-TEL-cKIT-N822K	0.36±0.006	0.11±0.018	0.04±0.001
BaF3-TEL-cKIT-D816V	＞10	0.42±0.0057	0.67±0.015
BaF3-TEL-cKIT-T670I-V559D	5.2±1.1	0.007±0.001	0.073±0.004
BaF3-TEL-cKIT-V559D-V654A	0.70±0.16	0.006±0.0006	0.36±0.0001
GIST-T1 (cKIT wt)	0.027±0.0011	0.005±0.0002	0.004±0.0026
GIST-5R (cKIT-T670I)	8.3±0.32	0.021±0.0001	0.026±0.006

[a] All GI_{50} values were obtained by triple testing.

We also used ADP-Glo based biochemical activity assay with the purified kinase proteins to confirm the inhibition activities of compound **35** against cKIT and cKIT-T670I kinases. The results showed that **35** inhibited cKIT wt kinase with an IC_{50} of 33 nM, and inhibited cKIT T670I kinase with an IC_{50} of 99 nM (Figure 5).

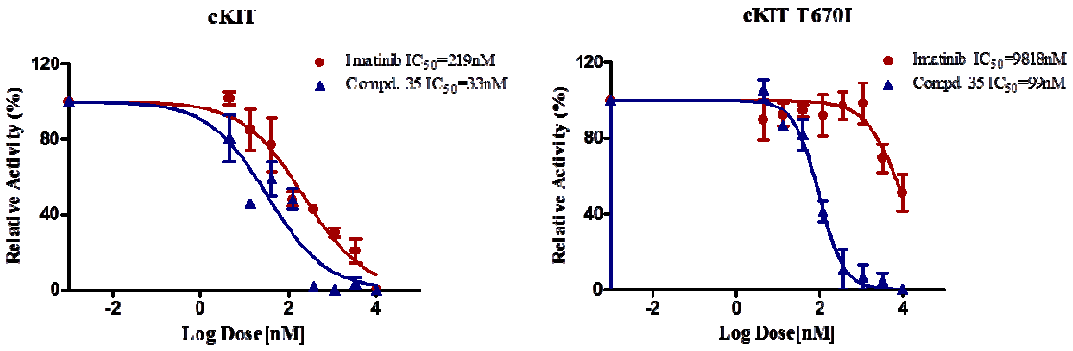

Figure 5. ADP-Glo biochemical characterization of compound **35** against cKIT wt/T670I kinases.

To better understand compound **35**'s selectivity, we examined its kinome wide selectivity profile with KinomeScan technology.[18] The results demonstrated that compound **35** bore a good selectivity (S score (1) = 0.03) in a panel of 468 kinases and mutants at 1 μM concentration. Besides high binding affinity to cKIT and cKIT-T670I kinases, it also displayed strong binding against CDKL2, CDKL3, CSF1R, DDR1, FLT3, FLT4, LOK, RET and PDGFRβ kinases (percent activity remaining less than 1% at 1 μM **35**) (Figure 6 and Supplemental Table 1). Given the fact that KinomeScan is a binding assay and sometimes cannot really reflect the compound's inhibitory activity, we then used TEL transformed BaF3 system to further test the on-target activity and selectivity of **35** against other potential off-targets revealed by KinomeScan assay (Table 4). The data showed that compound **35** also potently inhibited PDGFRβ (GI_{50}: 0.005 μM) and displayed apparent activity against FLT3 (GI_{50}: 0.099 μM), FLT4 (GI_{50}: 0.24 μM), CSF1R (GI_{50}: 0.11 μM) as well as RET (GI_{50}: 0.12 μM). This is not surprising since cKIT, FLT3, CSF1R and PDGFR kinases all belong to the type III receptor tyrosine kinase family and the ATP binding pocket of these kinases are highly conserved.

A

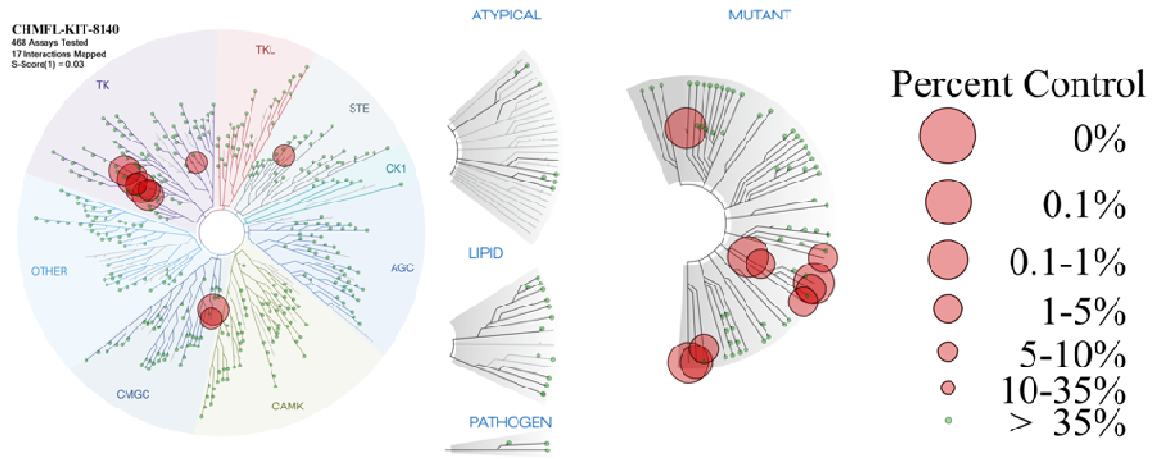

B

Targets	CDKL2	CDKL3	CSF1R	FLT3	FLT4	LOK	RET	PDGFRb
% activity remaining	0	0.3	0.05	0.85	0	0.35	0	0

Figure 6. Kinome wide selectivity profiling of compound **35**. (A) KinomeScan profiling of compound **35** at a concentration of 1 μM against 468 kinases and mutants. (B) Kinases that remained activity less than 1% of control in the presence of 1 μM **35**.

Table 4. Anti-proliferative Effects of Compound **35** against KinaseTargets Revealed from the KinomeScan Profiling in Isogenic BaF3 Cell Lines[a]

Cell line	GI_{50} (μM)
BaF3-TEL-CSF1R	0.11±0.006
BaF3-TEL-FLT3	0.099±0.0011
BaF3-TEL-FLT4	0.24±0.01
BaF3-TEL-RET	0.12±0.0057
BaF3-TEL-PDGFRβ	0.005±0.0007

[a] All GI_{50} values were obtained by triple testing.

We next investigated compound **35**'s effects on the cKIT mediated signaling pathways in cKIT wt and cKIT T670I driven GIST cell lines GIST-T1 and GIST-5R, respectively (Figure 7). As the results demonstrated, compound **35** completely blocked cKIT pY703, pY719, pY823 auto-phosphorylation sites in GIST-T1 cells at the concentration of 100 nM, and also remarkably inhibited downstream signaling mediators pAKT (T308, S473), pS6 (S235/236), pERK (T202/204) (EC_{50} less than 100 nM). Compound **1** displayed similar effect on the signaling pathways, which further proved **35**'s cKIT kinase inhibitory activity. In the Imatinib-resistant cell line GIST-5R (cKIT T670I), **35** also significantly affected cKIT pY703, pY719, pY823 auto-phosphorylation sites and downstream mediator phosphorylation (EC_{50} less than 100 nM). Not surprisingly, compound **1**'s inhibitory effect was much weaker even at the concentration of 1 μM. In addition, compound **35** started to induce dose-dependent cell apoptotic death (by examining the cleaved PARP) in both GIST-T1 and GIST-5R cells from the concentration of 30 nM at 24 h, while at the same time point compound **1** did not cause apparent apoptosis in both cells (Figure 8).

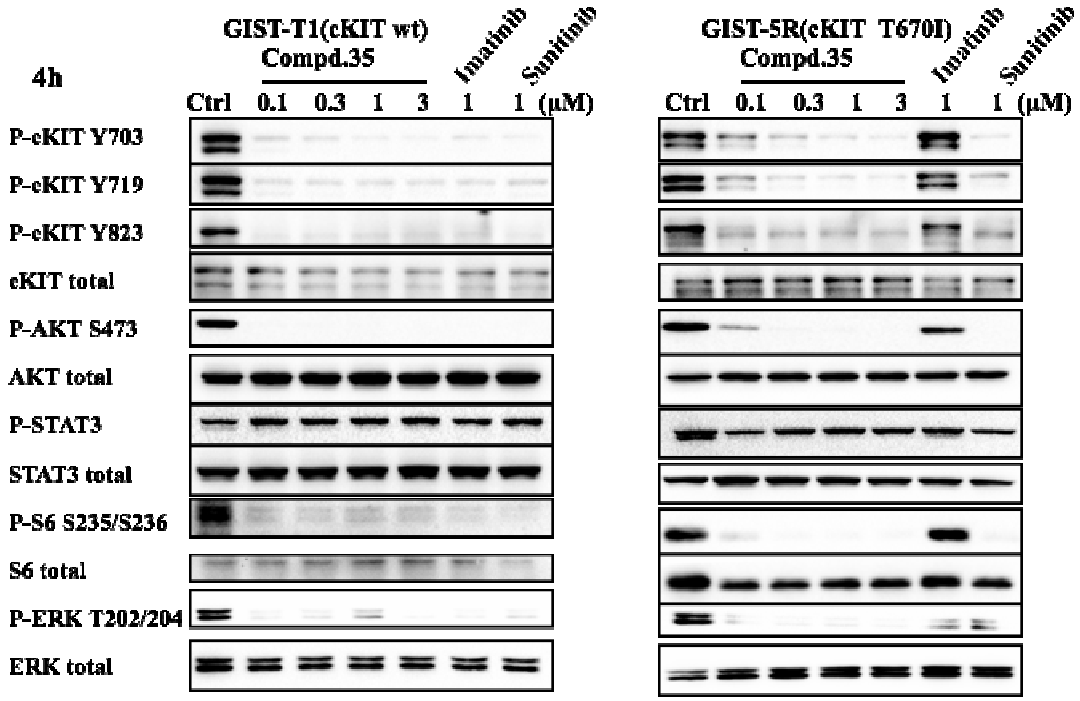

Figure 7. Effect of compounds **1**, **2** and **35** on cKIT mediated signaling pathways in GIST-T1 and GIST-5R cancer cell lines.

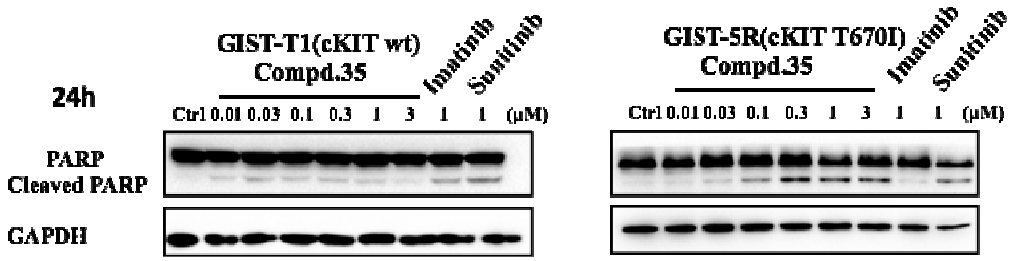

Figure 8. Effect of compounds **1**, **2** and **35** on induction of apoptosis in GIST-T1 and GIST-5R cell lines.

In Vivo PK/PD Evaluation.

The PK properties of compound **35** were evaluated using rats model (Table 5). With the intravenous injection compound **35** exhibited a $T_{1/2}$ of 2.04 h and Cmax of 2563.2 ng/mL. However, in the oral administration there was almost no absorption, which prevented **35** from the oral application in the animal model. We also tested the solubility of compound **35** and the data showed that in the PBS buffer (pH=7.4) it was 22.8±0.2 μg/mL (about 35 μM) while in the pure water it was 50.8±4.7 μg/mL (about 78 μM). This indicated that **35** should be fully dissolved at the concentrations we used in the in vitro studies.

Table 5. Pharmacokinetic Study of Compound **35** on Sprague Dawley Rats

	$T_{1/2}$ (h)	T_{max} (h)	C_{max} (ng/mL)	$AUC_{(0-t)}$ (ng/mL*h)	$AUC_{(0-\infty)}$ (ng/mL*h)	Vz (L/kg)	CLz (L/h/kg)	$MRT_{(0-\infty)}$ (h)
iv 1 mg/kg mean	2.04	0.017	2563.2	377.2	384.9	7.91	2.76	0.78
SD (n = 3)	0.86	0.0	825.4	100.1	105.0	3.11	0.89	0.11

We finally tested the antitumor efficacy of compound **35** in BaF3-TEL-cKIT-T670I cells inoculated xenograft mouse model. Based on the PK data, we chose the IP injection method. The results demonstrated that none of the 25, 50 and 100 mg/kg/day treatment affected the mice body weight (Figure 9A). During 10 days of continuous treatment, compound **35** dose-dependently inhibited the growth of the BaF3-TEL-cKIT-T670I tumor progression and a dosage of 100 mg/kg/day exhibited 47.7% TGI (tumor growth inhibition) (Figure 9B-D). The immunohistochemistry stain showed that in the tumors the inhibitor dose-dependently inhibited the tumor cell proliferation (examined by *K*i-67 staining) and induced apoptosis (examined by

TUNEL staining) (Figure 9E). Compared to compound **1**, which has been shown that it could promote but not suppress the cKIT T670I tumor growth, compound **35** demonstrated a proof of concept that a type II kinase inhibitor could effectively suppress the tumor progression.[19]

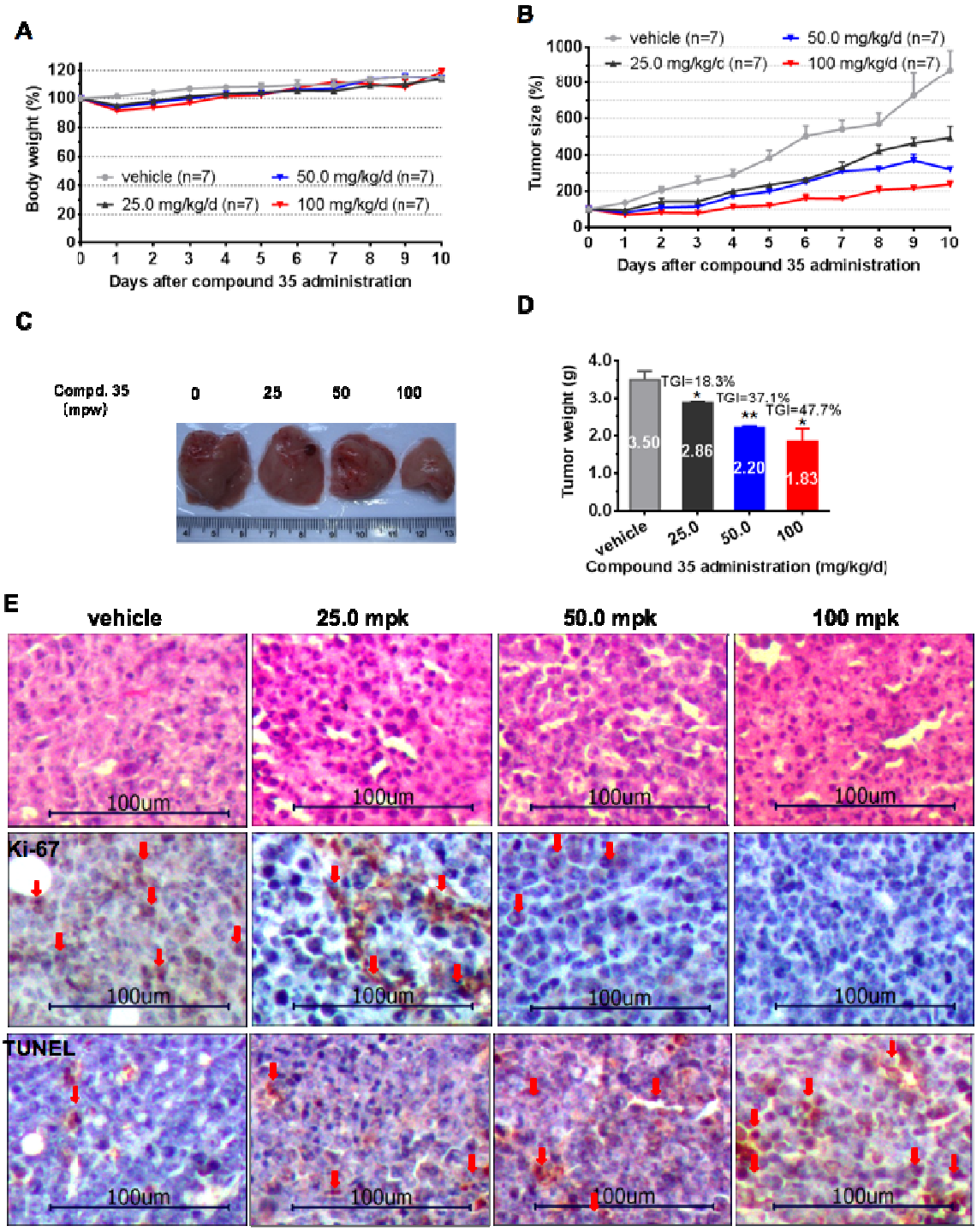

Figure 9. Compound **35**'s antitumor efficacy in BaF3-TEL-cKIT-T670I xenograft model. Female nu/nu mice bearing established BaF3-TEL-cKIT-T670I tumor xenografts were treated with compound **35** at 25, 50,100 mg/kg/d or vehicle. Daily IP administration was initiated when BaF3-TEL-cKIT-T670I tumors had reached a size of 200−400 mm^3. Each group contained seven animals. Data, mean ± SEM. (A) Body weight and (B) tumor size measurements from BaF3-TEL-cKIT-T670I xenograft mice after compound **35** administration. Initial body weight and tumor size were set as 100%. (C) Representative photographs of tumors in each group after 25, 50, 100 (mg/kg)/d compound **35** or vehicle treatment. (D) Comparison of the final tumor weight in each group after 10-day treatment period of **35**. Numbers in columns indicate the mean tumor weight in each group. ns, $p > 0.05$, (∗) $p < 0.05$, (∗∗) $p < 0.01$. (E) Representative micrographs of hematoxylin and eosin (HE), *K*i-67, and TUNEL staining of tumor tissues of **35** treatment groups in comparison with the vehicle group. Note the specific nuclear staining of cells with morphology consistent with proliferation and apoptosis (E, red arrow).

CHEMISTRY

The synthesis of urea compounds **7**, **9**, **11-36** started from nucleophilic substitution of 4-chloro-6,7-dimethoxyquinoline with 3-aminophenol which afforded compound **37** (Scheme 1). Boc-protected 3- or 4-aminopiperidine analogs (**39**) reacted with chloronitrobenzene derivatives (**38**) to provide **40** in two steps. Urea formation from the two precursors with triphosgene afforded compound **41**. Acidic deprotection of Boc group (**42**) and amide bond formation with corresponding acyl chlorides or carboxylic acids furnished the target compounds.

Scheme 1. Synthesis of Compounds 7, 9, 11-36[a]

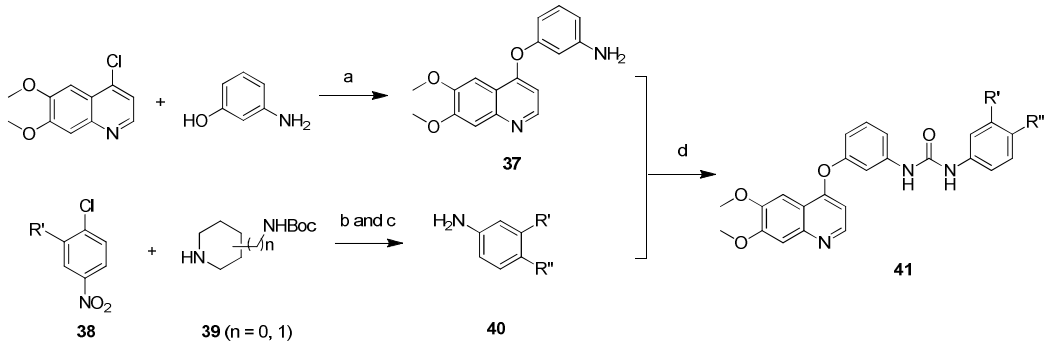

38a, R'=H
38b, R'=CF_3

39a = *tert*-butyl piperidin-3-ylcarbamate
39b = *tert*-butyl piperidin-4-ylcarbamate
39c = *tert*-butyl (piperidin-4-ylmethyl)carbamate

40a-41a, R' = H, R'' = *tert*-butyl piperidin-4-ylcarbamate
40b-41b, R' = CF_3, R'' = *tert*-butyl piperidin-3-ylcarbamate
40c-41c, R' = CF_3, R'' = *tert*-butyl (piperidin-4-ylmethyl)carbamate
40d-41d, R' = CF_3, R'' = *tert*-butyl piperidin-4-ylcarbamate

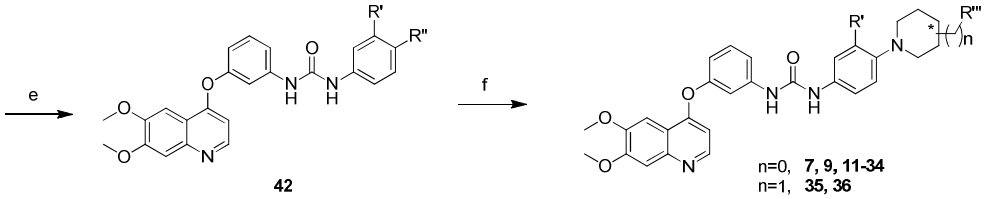

42a, R' = H, R'' = piperidin-4-amine hydrochloride
42b, R' = CF_3, R'' = piperidin-3-amine hydrochloride
42c, R' = CF_3, R'' = piperidin-4-ylmethanamine hydrochloride
42d, R' = CF_3, R'' = piperidin-4-amine hydrochloride

7, R' = CF_3, R''' = 4-propionamide
9, R' = H, R''' = 4-propionamide
11, R' = CF_3, R''' = 3-propionamide
12, R' = CF_3, R''' = 4-acetamide
13, R' = CF_3, R''' = 4-(3,3-dimethyl)butanamide
14, R' = CF_3, R''' = 4-(2-amino)acetamide hydrochloride
15, R' = CF_3, R''' = 4-[(*S*)-2-amino]propanamide hydrochloride
16, R' = CF_3, R''' = 4-[2-(dimethylamino)]acetamide
17, R' = CF_3, R''' = 4-cyclohex-1-enecarboxamide
18, R' = CF_3, R''' = 4-nicotinamide
19, R' = CF_3, R''' = 4-tetrahydro-2*H*-pyran-4-carboxamide
20, R' = CF_3, R''' = 4-(1-methyl)piperidine-4-carboxamide
21, R' = CF_3, R''' = 4-(1-ethyl)piperidine-4-carboxamide
22, R' = CF_3, R''' = 4-(1-acetyl)piperidine-4-carboxamide
23, R' = CF_3, R''' = 4-(1-cyclopropanecarbonyl)piperidine-4-carboxamide
24, R' = CF_3, R''' = 4-(1-tert butyl carboxylate)piperidine-3-carboxamide
25, R' = CF_3, R''' = 4-(2-methyl)piperidine-4-carboxamide hydrochloride
26, R' = CF_3, R''' = 4-[2-(piperidin-1-yl)]acetamide
27, R' = CF_3, R''' = 4-[2-(3-methylpiperidin-1-yl)]acetamide
28, R' = CF_3, R''' = 4-[3-(piperidin-1-yl)]propanamide
29, R' = CF_3, R''' = 4-[3-(1-methylpiperidin-2-yl)]propanamide
30, R' = CF_3, R''' = 4-(3-morpholino)propanamide
31, R' = CF_3, R''' = 4-methanesulfonamide
32, R' = CF_3, R''' = 4-ethanesulfonamide
33, R' = CF_3, R''' = 4-(1-propane)sulfonamide
34, R' = CF_3, R''' = 4-cyclopropanesulfonamide
35, R' = CF_3, R''' = 4-(*N*-propionamide)methanamine
36, R' = CF_3, R''' = 4-[*N*-3-(1-methylpiperidin-2-yl)propionamide]methanamine

[a]Reagents and conditions: (a) *t*BuOK, K_2CO_3, DMSO, 100 °C, 12 h; (b) K_2CO_3, DMF, 100 °C, 8 h; (c) H_2, 10% Pd/C, MeOH, rt, 3 h; (d) triphosgene, Et_3N, DMAP, DCM, 0 °C to rt, 1 h; (e) 4 M HCl in ethyl acetate, rt, 1 h; (f) for **7**, **9**, **11-13** and **31-35**: acyl chloride, Et_3N, DMF, -50 °C, 5 min; for **16-24**, **26-30** and **36**: carboxylic acid, HATU, Et_3N, DMF, rt, overnight; for **14-15** and **25**: (i) carboxylic acid, HATU, Et_3N, DMF, rt, overnight; (ii) 4 M HCl in ethyl acetate, rt, 1 h.

Compound **10** was prepared via a similar approach in different reaction order (Scheme 2). The nucleophilic substitution of trifluoromethyl substituted chloronitrobenzene (**38b**) and Boc-protected 4-aminopiperidine (**39b**) was followed by Boc-deprotection (**44**) and connection with **37** through triphosgene. Hydrogenation of the nitro group in **45** provided the amine moiety, which then readily reacted with the propionyl chloride.

Scheme 2. Synthesis of Compound 10[a]

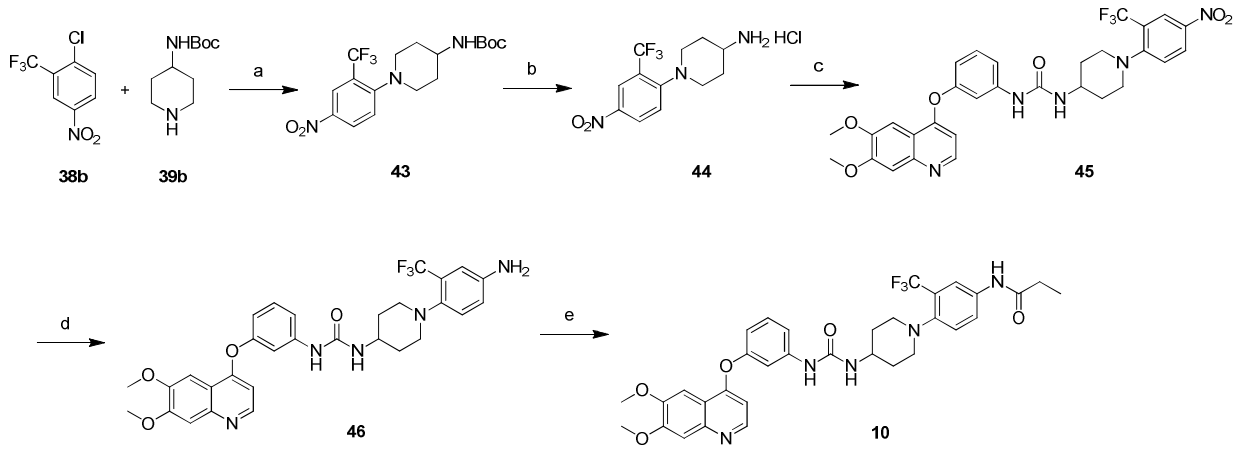

[a]Reagents and conditions: (a) K_2CO_3, DMF, 100 °C, 8 h; (b) 4 M HCl in ethyl acetate, rt, 1 h; (c) **37**, triphodgene, Et_3N, DMAP, DCM, 0 °C to rt, 1 h; (d) H_2, 10% Pd/C, MeOH, rt, 8 h; (e) propionyl chloride, Et_3N, DMF, -50 °C, 5 min.

The synthesis of compound **8** that bears a cyclopropane-1,1-dicarboxamide moiety at the **R1** position was achieved by amidation of **37** with 1-(methoxycarbonyl)cyclopropanecarboxylic acid, which was followed by methyl ester hydrolysis of **47** and coupling reaction of **48** with **40d**. Final Boc deprotection and acylation afforded compound **8** (Scheme 3).

Scheme 3. Synthesis of Compound 8[a]

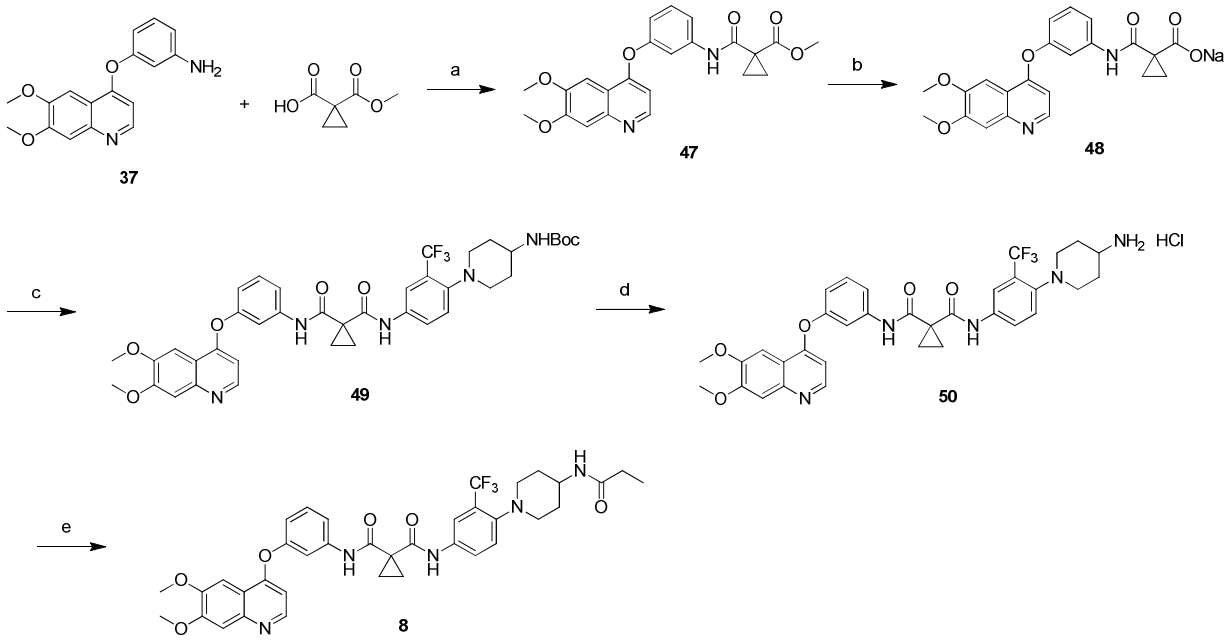

[a]Reagents and conditions: (a) HATU, DIPEA, DMF, rt, overnight; (b) 1.0 M NaOH, MeOH, reflux, 2 h; (c) **40d**, HATU, DIPEA, DMF, rt, overnight; (d) 4 M HCl in ethyl acetate, rt, 1 h; (e) propionyl chloride, Et_3N, DMF, -50 °C, 5 min.

CONCLUSIONS

In summary, we have discovered a new quinoline scaffold based highly potent type II kinase inhibitor compound **35**, which possessed strong inhibitory activities against both cKIT wt GIST cancer cells (GIST-T1) and cKIT T670I gatekeeper mutant cells (GIST-5R). The compound strongly inhibited cKIT mediated signaling pathways and dose-dependently induced apoptosis. Although **35** displayed good anti-tumor efficacies in the cKIT T670I mutant cells mediated xenograft mouse models, the poor oral PK profile prevented it from further development. Further medicinal chemistry effort is needed to improve the PK profile of this series of compounds. We believe compound **35** will be a useful pharmacological tool for exploration of the cKIT kinase gatekeeper T670I mutant mediated pathology in GISTs.

EXPERIMENTAL SECTION

Chemistry. All reagents and solvents were purchased from commercial sources and used as obtained. ^{1}H NMR and ^{13}C NMR spectra were recorded with a Bruker 400 NMR spectrometer and referenced to deuterium dimethyl sulfoxide (DMSO-d_6) or deuterium chloroform ($CDCl_3$). Chemical shifts are expressed in ppm. In the NMR tabulation, s indicates singlet; d, doublet; t, triplet; q, quartet; m, multiplet; and br, broad peak. LC/MS were performed on an Agilent 6224 TOF using an ESI source coupled to an Agilent 1260 Infinity HPLC system operating in reverse mode with an Agilent Eclipse Plus C18 1.8 μm 3.0×50 mm column. Flash column chromatography was conducted using silica gel (Silicycle 40−64 μm). The purities of all compounds were determined to be above 95% by HPLC.

Compounds **7-13** and **31-35** were prepared following the synthetic procedure of **7**.

N-(1-(4-(3-(3-((6,7-Dimethoxyquinolin-4-yl)oxy)phenyl)ureido)-2-(trifluoromethyl)phenyl)piperidin-4-yl)propionamide (7) To a solution of **42d** (30.0 mg, 0.057 mmol), Et_3N (0.039 mL, 0.171 mmol) in anhydrous DMF (0.5 mL) at -50 °C under Ar was added propionyl chloride (6.3 mg, 0.0682mmol). After being stirred at -50 °C for 5 min., the reaction mixture was quenched with water and warmed up to room temperature. The mixture was diluted with ethyl acetate and washed with water and brine. The organic phase was dried with $MgSO_4$, filtered, and concentrated under vacuum to give the residue which was purified by silica gel flash chromatography with dichloromethane/methanol (10:1) to afford the title compound **7** as a white solid (8.5 mg, 25%). ^{1}H NMR (400 MHz, DMSO-d_6) δ 9.02 (s, 2H), 8.51 (d, J = 5.2 Hz, 1H), 7.88 (d, J = 2.2 Hz, 1H), 7.77 (d, J = 7.8 Hz, 1H), 7.60 – 7.53 (m, 2H), 7.50 (d, J = 8.9 Hz, 2H), 7.47 – 7.39 (m, 2H), 7.28 (d, J = 8.0 Hz, 1H), 6.90 (dd, J = 8.0, 1.9 Hz, 1H), 6.55 (d, J = 5.2 Hz, 1H), 3.95 (s, 6H), 3.70 – 3.64 (m, 1H), 2.87 – 2.84 (m, 2H), 2.79 – 2.74 (m,

2H), 2.07 (q, J = 7.6 Hz, 2H), 1.80 – 1.77 (m, 2H), 1.52 – 1.46 (m, 2H), 1.00 (t, J = 7.6 Hz, 3H). ^{13}C NMR (101 MHz, DMSO-d_6) δ 172.55, 159.90, 154.98, 152.99, 149.86, 149.32, 147.26, 141.95, 137.14, 130.96, 125.78, 123.45, 115.73, 114.52, 110.86, 108.34, 104.14, 99.52, 56.16, 53.23, 45.73, 32.77, 29.03, 10.44. LC-MS (ESI, m/z): calcd for $C_{33}H_{35}F_3N_5O_5$ $[M+H]^+$: 638.2590; found: 638.2593.

*N-(3-((6,7-dimethoxyquinolin-4-yl)oxy)phenyl)-N-(4-(4-propionamidopiperidin-1-yl)-3-(trifluoromethyl)phenyl)cyclopropane-1,1-dicarboxamide (**8**)* (white solid , 19% yield). ^{1}H NMR (400 MHz, DMSO-d_6) δ 10.23 (s, 1H), 10.18 (s, 1H), 8.51 (d, J = 5.1 Hz, 1H), 8.03 (d, J = 5.6 Hz, 1H), 7.80 – 7.75 (m, 2H), 7.66 (d, J = 1.0 Hz, 1H), 7.61 (d, J = 8.4 Hz, 1H), 7.51 (dd, J = 12.8, 7.2 Hz, 2H), 7.41 (d, J = 0.5 Hz, 1H), 7.09 (d, J = 4.0 Hz, 1H), 7.00 (d, J = 7.6 Hz, 1H), 6.55 (d, J = 5.2 Hz, 1H), 3.96 (s, 3H), 3.93 (s, 3H), 3.73 – 3.64 (m, 1H), 2.86 – 2.74 (m, 4H), 2.09 – 2.04 (m, 2H), 1.82 – 1.76 (m, 2H), 1.57 – 1.44 (m, 4H), 1.00 (t, J = 7.4 Hz, 3H). LC-MS (ESI, m/z): calcd for $C_{37}H_{39}F_3N_5O_6$ $[M+H]^+$: 706.2852; found: 706.2867.

*N-(1-(4-(3-(3-((6,7-dimethoxyquinolin-4-yl)oxy)phenyl)ureido)phenyl)piperidin-4-yl)propionamide (**9**)* (white solid, 29 % yield). ^{1}H NMR (400 MHz, DMSO-d_6) δ 9.25 (s, 1H), 8.88 (s, 1H), 8.51 (d, J = 4.9 Hz, 1H), 7.74 (d, J = 7.6 Hz, 1H), 7.56 (s, 1H), 7.51 (s, 1H), 7.44 – 7.35 (m, 2H), 7.27 (t, J = 7.4 Hz, 3H), 6.85 (t, J = 9.1 Hz, 3H), 6.55 (d, J = 5.0 Hz, 1H), 3.95 (s, 6H), 3.73 – 3.60 (m, 1H), 3.54 – 3.50 (m, 2H), 2.72 – 2.66 (m, 2H), 2.05 – 2.00 (m, 2H), 1.81 – 1.78 (m, 2H), 1.52 – 1.42 (m, 2H), 0.99 (t, J = 7.5 Hz, 3H). LC-MS (ESI, m/z): calcd for $C_{32}H_{36}N_5O_5$ $[M+H]^+$: 570.2716; found: 570.2733.

*N-(4-(4-(3-(3-((6,7-dimethoxyquinolin-4-yl)oxy)phenyl)ureido)piperidin-1-yl)-3-(trifluoromethyl)phenyl)propionamide (**10**)* (white solid, 45 % yield). ^{1}H NMR (400 MHz, DMSO-d_6) δ 10.11 (s, 1H), 8.78 (s, 1H), 8.50 (d, J = 5.0 Hz, 1H), 8.00 (d, J = 1.5 Hz, 1H), 7.78

(d, J = 7.2 Hz, 1H), 7.59 – 7.47 (m, 2H), 7.41 (s, 1H), 7.39 – 7.31 (m, 1H), 7.19 (d, J = 7.8 Hz, 1H), 6.86 – 6.75 (m, 1H), 6.54 (d, J = 5.0 Hz, 1H), 6.48 (d, J = 6.1 Hz, 1H), 3.96 (s, 6H), 3.65 – 3.57 (m, 1H), 2.94 – 2.86 (m, 2H), 2.83 – 2.73 (m, 2H), 2.33 (dd, J = 14.5, 7.1 Hz, 2H), 1.95 – 1.87 (m, 2H), 1.59 – 1.47 (m, 2H), 1.08 (t, J = 7.5 Hz, 3H). ^{13}C NMR (101 MHz, DMSO-d_6) δ 172.69, 159.96, 155.01, 154.90, 153.05, 149.32, 147.00, 143.01, 136.92, 130.75, 125.99, 123.90, 117.35, 115.84,114.86, 113.37, 110.03, 108.36, 104.21, 99.55, 56.19, 56.14, 52.91, 33.16, 29.93, 10.00. LC-MS (ESI, m/z): calcd for $C_{33}H_{35}F_3N_5O_5$ $[M+H]^+$: 638.2590; found: 638.2599.

N-(1-(4-(3-(3-((6,7-dimethoxyquinolin-4-yl)oxy)phenyl)ureido)-2-(trifluoromethyl)phenyl)piperidin-3-yl)propionamide ***(11)*** (yellow solid, 41% yield). ^{1}H NMR (400 MHz, DMSO-d_6) δ 9.34 (s, 2H), 8.51 (d, J = 4.5 Hz, 1H), 7.89 (s, 1H), 7.59 (s, 3H), 7.52 (s, 1H), 7.47 – 7.36 (m, 3H), 7.31 (d, J = 6.9 Hz, 2H), 6.89 (d, J = 7.2 Hz, 1H), 6.56 (d, J = 4.5 Hz, 1H), 3.96 (d, J = 5.3 Hz, 6H), 3.86 – 3.83 (m, 1H), 3.10 – 3.07 (m, 1H), 2.96 – 2.92 (m, 1H), 2.80 – 2.75 (m, 1H), 2.62 – 2.57 (m, 1H), 2.07 (q, J = 7.3 Hz, 2H), 1.80 – 1.72 (m, 2H), 1.61 – 1.52 (m, 1H), 1.33 – 1.29 (m, 1H), 0.98 (t, J = 7.4 Hz, 3H). LC-MS (ESI, m/z): calcd for $C_{33}H_{35}F_3N_5O_5$ $[M+H]^+$: 638.2590; found: 638.2591.

N-(1-(4-(3-(3-((6,7-dimethoxyquinolin-4-yl)oxy)phenyl)ureido)-2-(trifluoromethyl)phenyl)piperidin-4-yl)acetamide ***(12)*** (white solid, 40% yield). ^{1}H NMR (400 MHz, DMSO-d_6) δ 9.56 (s, 2H), 8.56 – 8.48 (m, 1H), 7.88 (d, J = 10.2 Hz, 2H), 7.53 (dt, J = 16.7, 4.3 Hz, 4H), 7.46 – 7.39 (m, 2H), 7.29 (dd, J = 7.6, 1.1 Hz, 1H), 6.89 (dd, J = 7.8, 1.1 Hz, 1H), 6.57 (d, J = 5.1 Hz, 1H), 3.96 (s, 6H), 3.75 – 3.62 (m, 1H), 2.88 – 2.85 (m, 2H), 2.81 – 2.70 (m, 2H), 1.81 (s, 3H), 1.80 – 1.77 (m, 2H), 1.57 – 1.45 (m, 2H). LC-MS (ESI, m/z): calcd for $C_{32}H_{33}F_3N_5O_5$ $[M+H]^+$: 624.2434; found: 624.2452.

N-(1-(4-(3-(3-((6,7-dimethoxyquinolin-4-yl)oxy)phenyl)ureido)-2-(trifluoromethyl)phenyl)piperidin-4-yl)-3,3-dimethylbutanamide ***(13)*** (white solid, 43% yield). ^{1}H NMR (400 MHz, DMSO-d_6) δ 9.69 (s, 2H), 8.51 (d, J = 8.0 Hz, 1H), 7.91 (d, J = 1.0 Hz, 1H), 7.75 (dd, J = 9.6, 2.9 Hz, 1H), 7.59 – 7.49 (m, 4H), 7.45 – 7.40 (m, 2H), 7.28 (dd, J = 8.3, 3.0 Hz, 1H), 6.88 (dd, J = 9.2, 3.7 Hz, 1H), 6.55 – 6.53 (m, 1H), 3.96 (s, 6H), 3.76 – 3.66 (m, 1H), 2.86 – 2.84 (m, 3H), 2.81 – 2.70 (m, 2H), 1.95 (s, 2H), 1.83 – 1.73 (m, 2H), 1.58 – 1.45 (m, 3H), 1.05 (s, 9H). LC-MS (ESI, m/z): calcd for $C_{36}H_{41}F_3N_5O_5$ $[M+H]^+$: 680.3060; found: 680.3062.

Compounds **14-15** and **25** were prepared following the synthetic procedure of **14**. Compounds **16-24**, **26-30** and **36** were prepared following the first step (amide bond formation) of the synthetic procedure of **14**.

2-Amino-N-(1-(4-(3-(3-((6,7-dimethoxyquinolin-4-yl)oxy)phenyl)ureido)-2-(trifluoromethyl)phenyl)piperidin-4-yl)acetamide hydrochloride ***(14)*** To a solution of **42d** (20 mg, 0.034 mmol), Et_3N (0.024 mL, 0.170 mmol) and HATU (20 mg, 0.052 mmol) in DMF (0.5 mL) was added (*tert*-butoxycarbonyl)glycine (10 mg, 0.052 mmol). The reaction mixture was stirred at room temperature overnight, and then diluted with ethyl acetate and washed with water and brine. The organic phase was separated and dried with $MgSO_4$, then filtered and concentrated. The residue was purified by silica gel flash chromatography with dichloromethane/methanol (10:1) to offer the Boc-prodected compound as a white solid (5.7 mg, 22%), which was then treated with 4.0 M HCl in ethyl acetate (5 mL) at room temperature for about 1 h. The reaction mixture was concentrated under vacuum to provide the product **14** as a white solid (5 mg, 97%). ^{1}H NMR (400 MHz, DMSO-d_6) δ 10.18 (s, 1H), 10.09 (s, 1H), 8.81 (d, J = 9.9 Hz, 1H), 8.61 – 8.52 (m, 1H), 8.18 (d, J = 11.1 Hz, 2H), 7.89 (d, J = 2.2 Hz, 1H), 7.78 (d, J = 2.7 Hz, 2H), 7.71 (d, J = 1.4 Hz, 1H), 7.60 – 7.49 (m, 3H), 7.38 (dd, J = 7.5, 2.7 Hz, 1H),

7.02 (dd, *J* = 9.8, 5.4 Hz, 1H), 6.91 (d, *J* = 5.0 Hz, 1H), 4.05 (s, 6H), 3.89 – 3.68 (m, 3H), 2.93 – 2.87 (m, 2H), 2.83 – 2.76 (m, 2H), 1.87 – 1.79 (m, 2H), 1.59 – 1.49 (m, 2H). LC-MS (ESI, m/z): calcd for $C_{32}H_{34}F_3N_6O_5$ $[M+H]^+$: 639.2543; found: 639.2557.

(R)-2-amino-N-(1-(4-(3-(3-((6,7-dimethoxyquinolin-4-yl)oxy)phenyl)ureido)-2-(trifluoromethyl)phenyl)piperidin-4-yl)propanamide hydrochloride ***(15)*** (white solid, 35% yield in two steps). ^{1}H NMR (400 MHz, DMSO-d_6) δ 10.18 (s, 1H), 10.08 (s, 1H), 8.87 – 8.76 (m, 1H), 8.57 (d, *J* = 7.3 Hz, 1H), 8.27 (d, *J* = 1.2 Hz, 2H), 7.89 (s, 1H), 7.78 (d, *J* = 0.6 Hz, 2H), 7.71 (d, *J* = 0.6 Hz, 1H), 7.61 – 7.48 (m, 2H), 7.40 – 7.34 (m, 1H), 7.07 – 6.98 (m, 1H), 6.95 – 6.85 (m, 1H), 4.05 (s, 6H), 3.88 – 3.69 (m, 2H), 3.04 (t, *J* = 11.4 Hz, 1H), 2.98 – 2.85 (m, 2H), 2.84 – 2.73 (m, 2H), 1.82 (dd, *J* = 18.1, 11.0 Hz, 2H), 1.64 – 1.49 (m, 2H), 1.28 – 1.15 (m, 3H). LC-MS (ESI, m/z): calcd for $C_{33}H_{36}F_3N_6O_5$ $[M+H]^+$: 653.2699; found: 653.2671.

N-(1-(4-(3-(3-((6,7-dimethoxyquinolin-4-yl)oxy)phenyl)ureido)-2-(trifluoromethyl)phenyl)piperidin-4-yl)-2-(dimethylamino)acetamide ***(16)*** (white solid, 42% yield). ^{1}H NMR (400 MHz, DMSO-d_6) δ 9.76 (s, 2H), 8.50 (d, *J* = 5.1 Hz, 1H), 8.06 (d, *J* = 13.1 Hz, 1H), 7.86 (s, 1H), 7.59 – 7.50 (m, 4H), 7.43 (t, *J* = 7.5 Hz, 2H), 7.28 (dd, *J* = 8.5, 2.4 Hz, 1H), 6.88 (dd, *J* = 8.3, 1.7 Hz, 1H), 6.55 (dd, *J* = 3.1, 1.9 Hz, 1H), 3.96 (s, 6H), 3.79 – 3.71 (m, 1H), 2.89 – 2.86 (m, 2H), 2.82 – 2.75 (m, 2H), 2.59 (s, 2H), 2.41 (s, 6H), 1.85 – 1.75 (m, 2H), 1.63 – 1.54 (m, 2H). LC-MS (ESI, m/z): calcd for $C_{34}H_{38}F_3N_6O_5$ $[M+H]^+$: 667.2856; found: 667.2873.

N-(1-(4-(3-(3-((6,7-dimethoxyquinolin-4-yl)oxy)phenyl)ureido)-2-(trifluoromethyl)phenyl)piperidin-4-yl)cyclohex-1-ene-1-carboxamide ***(17)*** (white solid, 19 yield). ^{1}H NMR (400 MHz, DMSO-d_6) δ 9.48 (d, *J* = 8.4 Hz, 2H), 8.55 (d, *J* = 4.9 Hz, 1H), 7.87 (s, 1H), 7.64 – 7.49 (m, 5H), 7.43 (d, *J* = 11.7 Hz, 2H), 7.29 (dd, *J* = 11.3, 3.5 Hz, 1H), 6.95 –

6.87 (m, 1H), 6.61 (d, J = 5.4 Hz, 1H), 6.52 (d, J = 5.3 Hz, 1H), 3.98 (s, 6H), 3.84 – 3.72 (m, 1H), 3.12 – 3.03 (m, 1H), 2.87 (dd, J = 12.4, 5.0 Hz, 2H), 2.78 (dt, J = 9.5, 4.3 Hz, 2H), 2.20 – 2.07 (m, 4H), 1.78 – 1.72 (m, 2H), 1.67 – 1.56 (m, 5H). LC-MS (ESI, m/z): calcd for $C_{37}H_{39}F_3N_5O_5$ $[M+H]^+$: 690.2903; found: 690.2929.

N-(1-(4-(3-(3-((6,7-dimethoxyquinolin-4-yl)oxy)phenyl)ureido)-2-(trifluoromethyl)phenyl)piperidin-4-yl)nicotinamide ***(18)*** (white solid, 39% yield). ^{1}H NMR (400 MHz, DMSO-d_6) δ 9.88 (d, J = 4.4 Hz, 2H), 9.04 (d, J = 1.1 Hz, 1H), 8.71 (d, J = 7.4 Hz, 1H), 8.61 (d, J = 8.2 Hz, 1H), 8.54 (dd, J = 3.5, 2.1 Hz, 1H), 8.23 (dd, J = 8.7, 3.5 Hz, 1H), 7.87 (d, J = 1.2 Hz, 1H), 7.62 – 7.48 (m, 5H), 7.44 (t, J = 5.7 Hz, 2H), 7.29 (dd, J = 8.3, 2.7 Hz, 1H), 6.90 (dd, J = 8.6, 1.7 Hz, 1H), 6.59 – 6.57 (m, 1H), 3.97 (s, 6H), 2.95 – 2.81 (m, 5H), 1.91 – 1.85 (m, 2H), 1.81 – 1.71 (m, 2H). LC-MS (ESI, m/z): calcd for $C_{36}H_{34}F_3N_6O_5$ $[M+H]^+$: 687.2543; found: 687.2570.

N-(1-(4-(3-(3-((6,7-dimethoxyquinolin-4-yl)oxy)phenyl)ureido)-2-(trifluoromethyl)phenyl)piperidin-4-yl)tetrahydro-2H-pyran-4-carboxamide ***(19)*** (light yellow solid, 32%yield). ^{1}H NMR (400 MHz, DMSO-d_6) δ 9.45 (s, 2H), 8.51 – 8.50 (m, 1H), 7.87 (s, 1H), 7.79 (dd, J = 7.5, 0.5 Hz, 1H), 7.57 (d, J = 10.0 Hz, 2H), 7.53 – 7.46 (m, 2H), 7.43 (d, J = 10.3 Hz, 2H), 7.33 – 7.25 (m, 1H), 6.88 (dd, J = 8.1, 0.9 Hz, 1H), 6.57 – 6.52 (m, 1H), 3.96 (s, 6H), 3.86 (dd, J = 11.5, 0.9 Hz, 2H), 3.74 – 3.62 (m, 1H), 3.34 – 3.25 (m, 2H), 2.90 – 2.85 (m, 2H), 2.78 – 2.72 (m, 2H), 2.37 – 2.31 (m, 1H), 1.81 – 1.73 (m, 2H), 1.62 – 1.50 (m, 6H). LC-MS (ESI, m/z): calcd for $C_{36}H_{39}F_3N_5O_6$ $[M+H]^+$: 694.2852; found: 694.2879.

N-(1-(4-(3-(3-((6,7-dimethoxyquinolin-4-yl)oxy)phenyl)ureido)-2-(trifluoromethyl)phenyl)piperidin-4-yl)-1-methylpiperidine-4-carboxamide ***(20)*** (white solid, 37% yield). ^{1}H NMR (400 MHz, DMSO-d_6) δ 9.46 (s, 2H), 8.50 (d, J = 4.9 Hz, 1H), 7.87 (d, J =

0.7 Hz, 2H), 7.57 (d, *J* = 9.9 Hz, 2H), 7.50 (d, *J* = 12.0 Hz, 2H), 7.46 – 7.37 (m, 2H), 7.28 (d, *J* = 8.8 Hz, 1H), 6.89 – 6.87 (m, 1H), 6.54 (d, *J* = 4.8 Hz, 1H), 3.95 (s, 6H), 3.72 – 3.64 (m, 1H), 3.16 – 3.05 (m, 2H), 2.88 – 2.85 (m, 3H), 2.78 – 2.72 (m, 2H), 2.54 (s, 6H), 2.25 – 2.15 (m, 2H), 1.79 – 1.70 (m, 6H), 1.57 – 1.49 (m, 2H). LC-MS (ESI, m/z): calcd for $C_{37}H_{42}F_3N_6O_5$ $[M+H]^+$: 707.3169; found: 707.3151.

*N-(1-(4-(3-(3-((6,7-dimethoxyquinolin-4-yl)oxy)phenyl)ureido)-2-(trifluoromethyl)phenyl)piperidin-4-yl)-1-ethylpiperidine-4-carboxamide (**21**)* (white solid, 35% yield). ^{1}H NMR (400 MHz, DMSO-d_6) δ 9.51 (s, 2H), 8.50 (d, *J* = 5.6 Hz, 1H), 7.87 – 7.83 (m, 2H), 7.57 (dd, *J* = 10.3, 0.8 Hz, 2H), 7.51 – 7.48 (m, 2H), 7.43 (dd, *J* = 10.4, 1.9 Hz, 2H), 7.29 – 7.25 (m, 1H), 6.89 (dd, *J* = 5.3, 4.2 Hz, 1H), 6.55 (dd, *J* = 4.8, 1.0 Hz, 1H), 3.96 (s, 6H), 3.72 – 3.63 (m, 1H), 3.03 – 2.97 (m, 2H), 2.90 – 2.85 (m, 2H), 2.78 – 2.72 (m, 2H), 2.38 – 2.32 (m, 3H), 2.27 – 2.12 (m, 3H), 1.81 – 1.68 (m, 6H), 1.57 – 1.48 (m, 2H). LC-MS (ESI, m/z): calcd for $C_{38}H_{44}F_3N_6O_5$ $[M+H]^+$: 721.3325; found: 721.3347.

*1-Acetyl-N-(1-(4-(3-(3-((6,7-dimethoxyquinolin-4-yl)oxy)phenyl)ureido)-2-(trifluoromethyl)phenyl)piperidin-4-yl)piperidine-4-carboxamide (**22**)* (white solid, 35% yield). ^{1}H NMR (400 MHz, DMSO-d_6) δ 9.23 (s, 2H), 8.51 (d, *J* = 4.9 Hz, 1H), 7.87 (d, *J* = 0.8 Hz, 1H), 7.83 (d, *J* = 7.8 Hz, 1H), 7.56 (d, *J* = 7.9 Hz, 2H), 7.50 (d, *J* = 9.1 Hz, 2H), 7.43 (d, *J* = 11.6 Hz, 2H), 7.28 (d, *J* = 8.4 Hz, 1H), 6.89 (dd, *J* = 7.7, 1.2 Hz, 1H), 6.58 – 6.52 (m, 1H), 4.39 – 4.33 (m, 1H), 3.95 (s, 6H), 3.84 – 3.80 (m, 1H), 3.72 – 3.64 (m, 1H), 3.05 – 2.97 (m, 1H), 2.89 – 2.85 (m, 2H), 2.78 – 2.73 (m, 2H), 2.37 – 2.30 (m, 1H), 1.99 (s, 3H), 1.79 – 1.75 (m, 2H), 1.70 – 1.63 (m, 2H), 1.52 – 1.47 (m, 3H), 1.41 – 1.33 (m, 1H). LC-MS (ESI, m/z): calcd for $C_{38}H_{42}F_3N_6O_6$ $[M+H]^+$: 735.3118; found: 735.3129.

1-(Cyclopropanecarbonyl)-N-(1-(4-(3-(3-((6,7-dimethoxyquinolin-4-yl)oxy)phenyl)ureido)-2-(trifluoromethyl)phenyl)piperidin-4-yl)piperidine-4-carboxamide ***(23)*** (white solid, 46% yield). ^{1}H NMR (400 MHz, DMSO-d_6) δ 9.35 (s, 2H), 8.53 (d, J = 4.1 Hz, 1H), 7.90 – 7.80 (m, 2H), 7.52 (dd, J = 18.4, 10.7 Hz, 4H), 7.46 – 7.39 (m, 2H), 7.29 (d, J = 8.1 Hz, 1H), 6.96 – 6.86 (m, 1H), 6.58 (d, J = 3.8 Hz, 1H), 4.41 – 4.20 (m, 2H), 3.97 (s, 6H), 3.75 – 3.62 (m, 1H), 3.16 – 3.01 (m, 1H), 2.87 (d, J = 9.8 Hz, 2H), 2.81 – 2.71 (m, 2H), 2.61 (dd, J = 14.4, 8.7 Hz, 1H), 2.38 (dd, J = 16.2, 10.8 Hz, 1H), 1.99 – 1.93 (m, 1H), 1.84 – 1.62 (m, 5H), 1.60 – 1.46 (m, 3H), 1.41 – 1.33 (m, 1H), 0.76 – 0.65 (m, 4H). LC-MS (ESI, m/z): calcd for $C_{40}H_{44}F_3N_6O_6$ $[M+H]^+$: 761.3274; found: 761.3286.

tert-Butyl 3-((1-(4-(3-(3-((6,7-Dimethoxyquinolin-4-yl)oxy)phenyl)ureido)-2-(trifluoromethyl)phenyl)piperidin-4-yl)carbamoyl)piperidine-1-carboxylate ***(24)*** (white solid, 45% yield). ^{1}H NMR (400 MHz, DMSO-d_6) δ 9.24 (s, 2H), 8.51 (d, J = 4.8 Hz, 1H), 7.93 – 7.85 (m, 1H), 7.61 – 7.54 (m, 2H), 7.50 (d, J = 10.0 Hz, 2H), 7.42 (t, J = 9.6 Hz, 2H), 7.32 – 7.25 (m, 1H), 6.89 (dd, J = 7.1, 0.8 Hz, 1H), 6.55 (d, J = 4.1 Hz, 1H), 3.96 (s, 6H), 3.89 – 3.83 (m, 1H), 3.71 – 3.65 (m, 1H), 2.90 – 2.85 (m, 3H), 2.80 – 2.72 (m, 5H), 2.24 – 2.17 (m, 1H), 1.85 – 1.74 (m, 3H), 1.67 – 1.64 (m, 1H), 1.58 – 1.47 (m, 4H). LC-MS (ESI, m/z): calcd for $C_{41}H_{48}F_3N_6O_7$ $[M+H]^+$: 793.3537; found: 793.3529.

N-(1-(4-(3-(3-((6,7-dimethoxyquinolin-4-yl)oxy)phenyl)ureido)-2-(trifluoromethyl)phenyl)piperidin-4-yl)-2-methylpiperidine-4-carboxamide hydrochloride ***(25)*** (white solid, 61% yield in two steps). 1H NMR (400 MHz, DMSO-d_6) δ 10.18 (s, 1H), 10.06 (s, 1H), 8.81 (d, J = 6.2 Hz, 1H), 8.03 – 7.94 (m, 1H), 7.87 (s, 1H), 7.77 (s, 2H), 7.73 – 7.68 (m, 1H), 7.53 (dd, J = 19.8, 8.7 Hz, 3H), 7.42 – 7.32 (m, 1H), 7.06 – 6.97 (m, 1H), 6.90 (d, J = 5.9 Hz, 1H), 4.05 (s, 6H), 3.72 – 3.62 (m, 1H), 3.47 – 3.41 (m, 1H), 3.32 – 3.20 (m, 1H), 3.14 – 3.04

(m, 1H), 2.91 – 2.83 (m, 2H), 2.75 – 2.73 (m, 2H), 1.84 – 1.71 (m, 4H), 1.61 – 1.46 (m, 3H). LC-MS (ESI, m/z): calcd for $C_{37}H_{42}F_3N_6O_5$ $[M+H]^+$: 707.3169; found: 707.3151.

N-(1-(4-(3-(3-((6,7-dimethoxyquinolin-4-yl)oxy)phenyl)ureido)-2-(trifluoromethyl)phenyl)piperidin-4-yl)-2-(piperidin-1-yl)acetamide ***(26)*** (white solid, 26% yield). ^{1}H NMR (400 MHz, DMSO-d_6) δ 9.36 (s, 2H), 8.51 (d, J = 4.6 Hz, 1H), 7.87 (d, J = 0.5 Hz, 1H), 7.61 – 7.47 (m, 4H), 7.43 (t, J = 6.1 Hz, 2H), 7.27 (d, J = 3.3 Hz, 1H), 6.93 – 6.85 (m, 1H), 6.60 – 6.51 (m, 1H), 3.96 (s, 6H), 3.79 – 3.72 (m, 1H), 3.03 – 2.73 (m, 6H), 2.48 – 2.40 (m, 2H), 1.84 – 1.73 (m, 2H), 1.64 – 1.56 (m, 6H), 1.43 – 1.36 (m, 2H). LC-MS (ESI, m/z): calcd for $C_{37}H_{42}F_3N_6O_5$ $[M+H]^+$: 707.3169; found: 707.3147.

N-(1-(4-(3-(3-((6,7-dimethoxyquinolin-4-yl)oxy)phenyl)ureido)-2-(trifluoromethyl)phenyl)piperidin-4-yl)-2-(3-methylpiperidin-1-yl)acetamide ***(27)*** (white solid, 19% yield). ^{1}H NMR (400 MHz, DMSO-d_6) δ 9.53 (s, 2H), 8.51 (d, J = 6.6 Hz, 1H), 7.86 (d, J = 0.8 Hz, 1H), 7.62 – 7.48 (m, 4H), 7.42 (d, J = 2.9 Hz, 2H), 7.28 (dd, J = 9.0, 3.6 Hz, 1H), 6.92 – 6.85 (m, 1H), 6.61 – 6.52 (m, 1H), 3.96 (s, 6H), 3.78 – 3.72 (m, 1H), 3.13 – 2.97 (m, 1H), 2.93 – 2.73 (m, 6H), 2.06 – 1.98 (m, 1H), 1.84 – 1.74 (m, 4H), 1.67 – 1.55 (m, 5H). LC-MS (ESI, m/z): calcd for $C_{38}H_{44}F_3N_6O_5$ $[M+H]^+$: 721.3325; found: 721.3319.

N-(1-(4-(3-(3-((6,7-dimethoxyquinolin-4-yl)oxy)phenyl)ureido)-2-(trifluoromethyl)phenyl)piperidin-4-yl)-3-(piperidin-1-yl)propanamide ***(28)*** (white solid, 18% yield). ^{1}H NMR (400 MHz, DMSO-d_6) δ 9.82 (d, J = 9.0 Hz, 2H), 8.53 (d, J = 4.0 Hz, 1H), 8.23 (dd, J = 10.1, 6.4 Hz, 1H), 7.86 (d, J = 1.7 Hz, 1H), 7.56 – 7.50 (m, 4H), 7.47 – 7.40 (m, 2H), 7.34 – 7.25 (m, 2H), 6.90 (d, J = 6.1 Hz, 1H), 6.59 (d, J = 4.1 Hz, 1H), 3.97 (s, 6H), 3.76 – 3.69 (m, 1H), 3.25 – 3.21 (m, 2H), 2.94 – 2.83 (m, 5H), 2.82 – 2.73 (m, 3H), 2.71 – 2.64 (m, 2H),

2.05 – 1.97 (m, 2H), 1.72 – 1.64 (m, 1H), 1.60 – 1.48 (m, 3H), 1.40 – 1.34 (m, 2H). LC-MS (ESI, m/z): calcd for $C_{38}H_{44}F_3N_6O_5$ $[M+H]^+$: 721.3325; found: 721.3347.

N-(1-(4-(3-(3-((6,7-dimethoxyquinolin-4-yl)oxy)phenyl)ureido)-2-(trifluoromethyl)phenyl)piperidin-4-yl)-3-(1-methylpiperidin-2-yl)propanamide ***(29)*** (white solid, 35% yield). ^{1}H NMR (400 MHz, DMSO-d_6) δ 9.50 (s, 2H), 8.50 (d, J = 4.7 Hz, 1H), 7.89 (dd, J = 11.1, 2.8 Hz, 2H), 7.57 (d, J = 9.4 Hz, 2H), 7.53 – 7.45 (m, 2H), 7.40 (d, J = 9.2 Hz, 2H), 7.29 (dd, J = 8.0, 0.4 Hz, 1H), 6.89 – 6.87 (m, 1H), 6.54 (d, J = 4.8 Hz, 1H), 3.96 (s, 6H), 3.69 – 3.66 (m, 1H), 3.02 – 2.94 (m, 1H), 2.86 (dd, J = 8.8, 1.7 Hz, 2H), 2.75 – 2.71 (m, 2H), 2.39 (s, 3H), 2.15 – 2.04 (m, 2H), 1.90 – 1.77 (m, 4H), 1.73 – 1.61 (m, 3H), 1.60 – 1.45 (m, 4H), 1.39 – 1.20 (m, 3H). LC-MS (ESI, m/z): calcd for $C_{39}H_{46}F_3N_6O_5$ $[M+H]^+$: 735.3482; found: 735.3463.

N-(1-(4-(3-(3-((6,7-dimethoxyquinolin-4-yl)oxy)phenyl)ureido)-2-(trifluoromethyl)phenyl)piperidin-4-yl)-3-morpholinopropanamide ***(30)*** (white solid, 40% yield). ^{1}H NMR (400 MHz, DMSO-d_6) δ 9.55 (s, 2H), 8.51 (d, J = 5.0 Hz, 1H), 8.00 (d, J = 7.2 Hz, 1H), 7.86 (d, J = 1.2 Hz, 1H), 7.57 (d, J = 12.5 Hz, 2H), 7.53 – 7.46 (m, 2H), 7.42 (t, J = 7.7 Hz, 2H), 7.29 (d, J = 7.7 Hz, 1H), 6.88 (d, J = 7.8 Hz, 1H), 6.56 (d, J = 5.0 Hz, 1H), 3.96 (s, 6H), 3.77 – 3.71 (m, 2H), 3.52 – 3.39 (m, 2H), 2.94 – 2.84 (m, 3H), 2.82 – 2.66 (m, 5H), 2.35 – 2.33 (m, 1H), 1.82 – 1.78 (m, 2H), 1.59 – 1.48 (m, 2H). LC-MS (ESI, m/z): calcd for $C_{37}H_{42}F_3N_6O_6$ $[M+H]^+$: 723.3118; found: 723.3130.

N-(1-(4-(3-(3-((6,7-dimethoxyquinolin-4-yl)oxy)phenyl)ureido)-2-(trifluoromethyl)phenyl)piperidin-4-yl)methanesulfonamide ***(31)*** (white solid, 31% yield). ^{1}H NMR (400 MHz, DMSO-d_6) δ 10.14 (s, 2H), 8.50 (d, J = 5.2 Hz, 1H), 7.90 (s, 1H), 7.67 – 7.60 (m, 1H), 7.58 (s, 1H), 7.52 (s, 1H), 7.49 – 7.32 (m, 4H), 7.18 – 7.13 (m, 1H), 6.86 (dd, J = 7.3, 0.8 Hz, 1H), 6.57 – 6.51 (m, 1H), 3.96 (s, 6H), 3.55 – 3.49 (m, 1H), 2.94 (s, 3H), 2.89 – 2.86 (m,

2H), 2.79 – 2.73 (m, 2H), 1.91 – 1.89 (m, 2H), 1.64 – 1.55 (m, 2H). LC-MS (ESI, m/z): calcd for $C_{31}H_{33}F_3N_5O_6S$ $[M+H]^+$: 660.2104; found: 660.2137.

N-(1-(4-(3-(3-((6,7-dimethoxyquinolin-4-yl)oxy)phenyl)ureido)-2-(trifluoromethyl)phenyl)piperidin-4-yl)ethanesulfonamide ***(32)*** (white solid, 23% yield). ^{1}H NMR (400 MHz, DMSO-d_6) δ 9.59 (s, 2H), 8.50 (d, J = 4.4 Hz, 1H), 7.87 (s, 1H), 7.57 (d, J = 12.3 Hz, 2H), 7.52 – 7.46 (m, 2H), 7.44 – 7.39 (m, 2H), 7.29 (dd, J = 8.0, 0.6 Hz, 1H), 7.20 (dd, J = 7.3, 1.3 Hz, 1H), 6.88 (dd, J = 7.3, 1.2 Hz, 1H), 6.56 – 6.51 (m, 1H), 3.96 (s, 6H), 3.25 – 3.19 (m, 1H), 3.06 – 2.99 (m, 2H), 2.88 – 2.85 (m, 2H), 2.78 – 2.71 (m, 2H), 1.91 – 1.83 (m, 2H), 1.64 – 1.55 (m, 2H), 1.24 – 1.16 (m, 3H). LC-MS (ESI, m/z): calcd for $C_{32}H_{35}F_3N_5O_6S$ $[M+H]^+$: 674.2260; found: 674.2267.

N-(1-(4-(3-(3-((6,7-dimethoxyquinolin-4-yl)oxy)phenyl)ureido)-2-(trifluoromethyl)phenyl)piperidin-4-yl)propane-1-sulfonamide ***(33)*** (white solid, 16% yield). ^{1}H NMR (400 MHz, DMSO-d_6) δ 9.51 (s, 2H), 8.50 (d, J = 3.4 Hz, 1H), 7.88 (d, J = 1.6 Hz, 1H), 7.62 – 7.54 (m, 2H), 7.49 (dd, J = 11.9, 8.2 Hz, 2H), 7.42 (t, J = 7.5 Hz, 2H), 7.33 – 7.28 (m, 1H), 7.22 – 7.16 (m, 1H), 6.88 (dd, J = 9.6, 4.8 Hz, 1H), 6.54 (d, J = 8.9 Hz, 1H), 3.96 (s, 6H), 3.29 – 3.18 (m, 1H), 3.05 – 2.96 (m, 2H), 2.91 – 2.83 (m, 2H), 2.78 – 2.71 (m, 2H), 1.90 – 1.84 (m, 2H), 1.72 – 1.66 (m, 2H), 1.62 – 1.54 (m, 2H), 1.01 – 0.97 (m, 3H). LC-MS (ESI, m/z): calcd for $C_{33}H_{37}F_3N_5O_6S$ $[M+H]^+$: 688.2417; found: 688.2450.

N-(1-(4-(3-(3-((6,7-dimethoxyquinolin-4-yl)oxy)phenyl)ureido)-2-(trifluoromethyl)phenyl)piperidin-4-yl)cyclopropanesulfonamide ***(34)*** (white solid, 63% yield). ^{1}H NMR (400 MHz, DMSO-d_6) δ 9.58 (s, 2H), 8.50 (d, J = 4.9 Hz, 1H), 7.96 (s, 1H), 7.87 (d, J = 1.1 Hz, 1H), 7.61 – 7.54 (m, 2H), 7.52 – 7.47 (m, 2H), 7.42 (t, J = 7.6 Hz, 2H), 7.32 – 7.26 (m, 1H), 7.21 (d, J = 8.4 Hz, 1H), 6.88 (dd, J = 8.4, 1.1 Hz, 1H), 6.55 (d, J = 4.9 Hz, 1H), 3.96 (s,

6H), 3.31 – 3.27 (m, 1H), 2.87 – 2.85 (m, 1H), 2.81 – 2.77 (m, 2H), 2.62 – 2.56 (m, 2H), 1.95 – 1.90 (m, 2H), 1.67 – 1.57 (m, 2H), 1.00 – 0.90 (m, 4H). LC-MS (ESI, m/z): calcd for $C_{33}H_{35}F_3N_5O_6S$ $[M+H]^+$: 686.2260; found: 686.2247.

N-((1-(4-(3-(3-((6,7-dimethoxyquinolin-4-yl)oxy)phenyl)ureido)-2-(trifluoromethyl)phenyl)piperidin-4-yl)methyl)propionamide ***(35)*** (white solid, 51% yield). ^{1}H NMR (400 MHz, DMSO-d_6) δ 9.28 (s, 2H), 8.54 (s, 1H), 7.84 (d, J = 21.4 Hz, 2H), 7.55 (d, J = 17.2 Hz, 3H), 7.43 (s, 3H), 7.30 (s, 1H), 6.90 (d, J = 6.3 Hz, 1H), 6.59 (s, 1H), 3.97 (s, 6H), 3.51 – 3.43 (m, 1H), 2.99 (s, 2H), 2.89 – 2.85 (m, 2H), 2.67 – 2.63 (m, 2H), 2.10 (d, J = 7.1 Hz, 2H), 1.70 – 1.67 (m, 2H), 1.53 – 1.49 (m, 1H), 1.01 (t, J = 6.9 Hz, 3H). LC-MS (ESI, m/z): calcd for $C_{34}H_{37}F_3N_5O_5$ $[M+H]^+$: 652.2747; found: 652.2757.

N-((1-(4-(3-(3-((6,7-dimethoxyquinolin-4-yl)oxy)phenyl)ureido)-2-(trifluoromethyl)phenyl)piperidin-4-yl)methyl)-3-(1-methylpiperidin-2-yl)propanamide ***(36)*** (white solid, 20% yield). ^{1}H NMR (400 MHz, DMSO-d_6) δ 9.77 (s, 1H), 9.71 (s, 1H), 8.50 (d, J = 4.5 Hz, 1H), 7.85 (s, 1H), 7.56 (d, J = 6.7 Hz, 2H), 7.52 (s, 1H), 7.46 – 7.42 (m, 3H), 7.29 (d, J = 5.9 Hz, 1H), 6.88 (d, J = 6.1 Hz, 1H), 6.56 (s, 1H), 3.96 (s, 6H), 3.56 – 3.47 (m, 1H), 3.10 (d, J = 3.5 Hz, 2H), 3.05 – 2.83 (m, 11H), 2.73 – 2.66 (m, 3H), 2.32 – 1.94 (m, 2H), 1.83 – 1.71 (m, 4H), 1.57 – 1.49 (m, 2H), 1.36 – 1.17 (m, 4H). LC-MS (ESI, m/z): calcd for $C_{40}H_{48}F_3N_6O_5$ $[M+H]^+$: 749.3638; found: 749.3651.

3-((6,7-Dimethoxyquinolin-4-yl)oxy)aniline ***(37)***. To a solution of 3-aminophenol (1.65 g, 13.4 mmol) in DMSO (15mL) was added *t*Bu-OK (1.51 g, 13.4 mmol) at room temperature. After stirring for 2 h, 4-chloro-6,7-dimethoxylquinoline (2.0 g, 8.9 mmol) and K_2CO_3 (738 mg, 5.34 mmol) were added, then the reaction mixture was heated to 100 °C and stirred for 12 h. After being cooled down to room temperature, the mixture was diluted with ethyl acetate and washed

with saturated $NaHCO_3$ (aq). The diluted mixture was then filtered through Celite to remove the emulsion. The organic phase was collected and washed with 1.0 M NaOH (aq) and brine, then dried with anhydrous $MgSO_4$. The filtrate was concentrated to give the residue which was purified by silica gel flash chromatography with dichloromethane/methanol (20:1) to afford the product **37** as a light yellow solid (2.48 g, 89% yield). ^{1}H NMR (400 MHz, DMSO-d_6) δ 8.49 (d, J = 5.2 Hz, 1H), 7.47 (s, 1H), 7.39 (s, 1H), 7.13 (t, J = 8.0 Hz, 1H), 6.55 - 6.49 (m, 2H), 6.38 – 6.34 (m, 2H), 5.39 (s, 2H), 3.94 (s, 3H) , 3.93 (s, 3H). ^{13}C NMR (101 MHz, DMSO-d_6) δ 160.13, 155.59, 152.93, 151.33, 149.70, 149.29, 146.91, 130.88, 111.51, 108.27, 107.83, 105.98, 104.14, 99.50, 56.13, 56.07. LC-MS (ESI, m/z): calcd for $C_{17}H_{17}N_2O_3$ $[M+H]^+$: 297.1239; found: 297.1243.

Compounds **40b**-**40d** were prepared following the synthetic procedure of **40a**.

*tert-Butyl (1-(4-aminophenyl)piperidin-4-yl)carbamate (**40a**)* To a solution of 1-chloro-4-nitrobenzene (2.0 g, 12.69 mmol) and K_2CO_3 (5.3 g, 38.09 mmol) in DMF (60 mL) was added *tert*-butyl piperidin-4-ylcarbamate (2.5 g, 12.69 mmol). The mixture was stirred at 100 °C for 8 h. The solvent was removed under vacuum after it was allowed to cool down to room temperature. The residue was dissolved in ethyl acetate, washed with water and brine, dried with $MgSO_4$, and then concentrated to afford the crude nitrobenzene product as a light yellow solid, which was used in the next step without further purification. LC-MS (ESI, m/z): 322.2906 $[M + H]^+$. To a solution of the crude nitrobenzene in methanol (50 mL) was added 10% Pd/C (2.0 g, 20% w/w) at room temperature. The reaction mixture was stirred under hydrogen balloon for 3 h, and then filtered through Celite. The filtrate was concentrated to give the residue which was purified by silica gel flash chromatography with dichloromethane/methanol (20:1) to afford compound **40a** as a brown solid (1.2 g, 32 % yield in two steps). ^{1}H NMR (400 MHz, DMSO-d_6)

δ 6.83 (d, J = 7.4 Hz, 1H), 6.69 (d, J = 7.8 Hz, 2H), 6.48 (d, J = 7.8 Hz, 2H), 4.64 (s, 2H), 3.33 – 3.28 (m, 3H), 2.55 – 2.51 (m, 2H), 1.83 – 1.71 (m, 2H), 1.55 – 1.45 (m, 2H), 1.40 (s, 9H). ^{13}C NMR (101 MHz, DMSO-d_6) δ 155.37, 143.15, 142.58, 119.11, 115.19, 77.93, 50.72, 47.87, 32.41, 28.73. LC-MS (ESI, m/z): calcd for $C_{16}H_{26}N_3O_2$ $[M+H]^+$: 292.2025; found: 292.2037.

*tert-Butyl 1-(4-amino-2-(trifluoromethyl)phenyl)piperidin-3-ylcarbamate (**40b**)* (light yellow solid, 91% yield). (white solid, 76% yield). ^{1}H NMR (400 MHz, DMSO-d_6) δ 7.16 (d, J = 7.7 Hz, 1H), 6.88 – 6.71 (m, 2H), 5.34 (s, 2H), 3.47 (d, J = 2.7 Hz, 1H), 2.86 (d, J = 8.4 Hz, 1H), 2.68 (d, J = 8.1 Hz, 1H), 2.39 (s, 1H), 1.76 (d, J = 8.8 Hz, 1H), 1.67 (d, J = 9.4 Hz, 1H), 1.53 (d, J = 5.3 Hz, 1H), 1.37 (s, 9H), 1.23 (d, J = 36.0 Hz, 1H). LC-MS (ESI, m/z): calcd for $C_{17}H_{25}F_3N_3O_2$ $[M+H]^+$: 360.1899; found: 360.1902.

*tert-Butyl (1-(4-amino-2-(trifluoromethyl)phenyl)piperidin-4-yl)methylcarbamate (**40c**)* (white solid, 69% yield). ^{1}H NMR (400 MHz, DMSO-d_6) δ 7.19 (d, J = 17.3 Hz, 1H), 6.80 (dd, J = 29.7, 13.0 Hz, 3H), 5.30 (s, 2H), 2.86 (d, J = 5.0 Hz, 2H), 2.77 (d, J = 9.4 Hz, 2H), 2.59 (t, J = 10.7 Hz, 2H), 1.63 (d, J = 11.2 Hz, 2H), 1.39 (s, 9H), 1.19 (dd, J = 21.4, 10.5 Hz, 2H). LC-MS (ESI, m/z): calcd for $C_{18}H_{27}F_3N_3O_2$ $[M+H]^+$: 374.2055; found: 374.2063.

*tert-Butyl (1-(4-amino-2-(trifluoromethyl)phenyl)piperidin-4-yl)carbamate (**40d**)* (yellow solid, 76% yield in two steps) ^{1}H NMR (400 MHz, DMSO-d_6) δ 7.24 (d, J = 8.5 Hz, 1H), 6.85 – 6.81 (m, 2H), 6.77 (d, J = 8.5 Hz, 1H), 5.32 (s, 2H), 3.36 – 3.27 (m, 1H), 2.78 – 2.76 (m, 2H), 2.69 – 2.66 (m, 2H), 1.76 – 1.73 (m, 2H), 1.57 – 1.43 (m, 2H), 1.39 (s, 9H). ^{13}C NMR (101 MHz, DMSO-d_6) δ 155.39, 146.72, 141.36, 126.80, 126.53, 126.06, 125.83, 123.35, 118.14, 111.17, 111.11, 77.88, 53.45, 47.70, 33.06, 28.72. LC-MS (ESI, m/z): calcd for $C_{17}H_{25}F_3N_3O_2$ $[M+H]^+$: 360.1899; found: 360.1910.

Compounds **41b**-**41d** were prepared following the synthetic procedure of **41a**.

*tert-Butyl (1-(4-(3-(3-((6,7-dimethoxyquinolin-4-yl)oxy)phenyl)ureido)phenyl) piperidin-4-yl)carbamate (**41a**)* To a solution of triphosgene (114 mg, 0.38 mmol) in anhydrous DCM (30 mL) was added a solution of **37** (300 mg, 0.97 mmol), Et_3N (0.2 mL, 1.46 mmol) and DMAP (12 mg, 0.09 mmol) in anhydrous DCM (10 mL) at 0 °C under argon. After stirring for 0.5 h, a solution of **40a** (283 mg, 0.97 mmol), Et_3N (0.2 mL, 1.46 mmol) and DMAP (12 mg, 0.09 mmol) in anhydrous DCM (10 mL) were added to the above reaction mixture at 0 °C under argon. Then the mixture was warmed to room temperature and stirred for 1 h. The reaction mixture was concentrated and the residue was purified by silica gel flash chromatography with dichloromethane/methanol (20:1) to afford the title compound **41a** as an off-white solid (418 mg, 69% yield). ^{1}H NMR (400 MHz, DMSO-d_6) δ 8.68 (s, 1H), 8.47 (d, J = 5.2 Hz, 1H), 8.39 (s, 1H), 7.57 (s, 1H), 7.47 (d, J = 1.9 Hz, 1H), 7.42 (s, 1H), 7.33 – 7.15 (m, 5H), 6.92 – 6.78 (m, 4H), 6.36 (d, J = 5.2 Hz, 1H), 3.96 (s, 6H), 3.51 (d, J = 12.4 Hz, 3H), 2.63 (t, J = 11.9 Hz, 3H), 2.07 (s, 3H), 1.80 (d, J = 1.7 Hz, 3H), 1.59 – 1.44 (m, 3H), 1.39 (s, 12H). LC-MS (ESI, m/z): calcd for $C_{34}H_{40}N_5O_6$ $[M+H]^+$: 614.2979; found: 614.2986.

*tert-Butyl1-(4-(3-(3-(6,7-dimethoxyquinolin-4-yloxy)phenyl)ureido)-2-(trifluoromethyl)phenyl)piperidin-3-ylcarbamate (**41b**)* (white solid, 57% yield). ^{1}H NMR (400 MHz, DMSO-d_6) δ 9.17 (s, 2H), 8.53 (d, J = 5.1 Hz, 1H), 8.33 (s, 1H), 7.86 (s, 1H), 7.29 (d, J = 7.6 Hz, 1H), 6.90 (d, J = 7.4 Hz, 1H), 6.71 (d, J = 18.7 Hz, 1H), 6.58 (d, J = 5.0 Hz, 1H), 3.97 (s, 6H), 3.66 – 3.41 (m, 3H), 2.96 (t, J = 17.1 Hz, 1H), 2.88 – 2.68 (m, 1H), 2.58 (d, J = 8.8 Hz, 2H), 2.44 (t, J = 13.0 Hz, 1H), 2.00 (dd, J = 23.7, 10.1 Hz, 1H), 1.89 – 1.66 (m, 3H), 1.56 (d, J = 22.9 Hz, 1H), 1.36 (s, 9H). LC-MS (ESI, m/z): calcd for $C_{35}H_{39}F_3N_5O_6$ $[M+H]^+$: 682.2852; found: 682.2869.

tert-Butyl(1-(4-(3-(3-(6,7-dimethoxyquinolin-4-yloxy)phenyl)ureido)-2-(trifluoromethyl) phenyl)piperidin-4-yl)methylcarbamate ***(41c)*** (white solid, 68% yield). ^{1}H NMR (400 MHz, DMSO-d_6) δ 9.21 (d, J = 8.9 Hz, 2H), 8.54 (d, J = 5.0 Hz, 1H), 8.32 (s, 1H), 7.86 (s, 1H), 7.56 (d, J = 17.4 Hz, 3H), 7.43 (t, J = 8.1 Hz, 3H), 7.29 (d, J = 7.4 Hz, 1H), 6.90 (d, J = 7.5 Hz, 2H), 6.60 (d, J = 5.1 Hz, 1H), 3.96 (s, 6H), 3.53 (d, J = 1.4 Hz, 2H), 2.87 (s, 4H), 2.65 (t, J = 10.5 Hz, 2H), 1.67 (d, J = 10.9 Hz, 2H), 1.47 (d, J = 6.1 Hz, 2H), 1.42 (d, J = 28.5 Hz, 9H). LC-MS (ESI, m/z): calcd for $C_{36}H_{41}F_3N_5O_6$ $[M+H]^+$: 696.3009; found: 696.3030.

tert-Butyl (1-(4-(3-(3-((6,7-dimethoxyquinolin-4-yl)oxy)phenyl)ureido)-2-(trifluoromethyl)phenyl)piperidin-4-yl)carbamate ***(41d)*** (yellow solid, 91% yield). ^{1}H NMR (400 MHz, DMSO-d_6) δ 8.97 (s, 2H), 8.51 (d, J = 5.1 Hz, 1H), 7.86 (s, 1H), 7.65 – 7.37 (m, 6H), 7.29 (d, J = 8.1 Hz, 1H), 6.88 (t, J = 7.6 Hz, 2H), 6.56 (d, J = 5.2 Hz, 1H), 3.95 (d, J = 6.4 Hz, 6H), 3.39 (s, 8H), 2.89 – 2.84 (m, 2H), 2.74 – 2.69 (m, 2H), 1.79 – 1.77 (m, 1H), 1.55 – 1.48 (m, 2H), 1.39 (s, 9H). ^{13}C NMR (101 MHz, DMSO-d_6) δ 159.92, 155.39, 154.98, 152.99, 149.85, 149.29, 147.28, 146.99, 141.94, 137.09, 130.93, 125.76, 123.43, 116.63, 115.74, 114.51, 110.88, 108.30, 104.13, 99.51, 77.95, 56.14, 55.35, 53.25, 47.57, 32.90, 28.72. LC-MS (ESI, m/z): calcd for $C_{35}H_{39}F_3N_5O_6$ $[M+H]^+$: 682.2852; found: 682.2861.

Compounds **42b-42d** were prepared following the synthetic procedure of **42a**.

1-(4-(4-Aminopiperidin-1-yl)phenyl)-3-(3-(6,7-dimethoxyquinolin-4-yloxy)phenyl)urea hydrochloride ***(42a)*** Compound **41a** (400 mg, 0.637 mmol) was dissolved in 4 M HCl in ethyl acetate (5 mL) at room temperature. The resulting mixture was stirred for 1 h, and then concentrated to afford the product **42a** as an off white solid (424 mg, 96%) which was used directly in the next step. ^{1}H NMR (400 MHz, DMSO-d_6) δ 9.99 (d, J = 3.7 Hz, 2H), 8.78 (d, J = 0.8 Hz, 1H), 8.66 (d, J = 0.4 Hz, 3H), 7.80 (dd, J = 34.2, 3.7 Hz, 4H), 7.58 (d, J = 17.0 Hz, 3H),

7.34 (dd, J = 30.4, 2.4 Hz, 2H), 6.74 (s, 1H), 4.03 (s, 6H), 3.70 – 3.66 (m, 4H), 3.55 – 3.53 (m, 1H), 2.30 – 2.25 (m, 4H), 2.05 (s, 3H). ^{13}C NMR (101 MHz, DMSO-d_6) δ 165.16, 156.51, 152.99, 151.60, 150.96, 143.16, 141.24, 139.97, 137.35, 136.42, 132.91, 122.91, 122.69, 118.83, 116.68, 115.53, 110.86, 103.34, 100.75, 100.13, 57.09, 56.92, 27.31, 15.19. LC-MS (ESI, m/z): calcd for $C_{29}H_{32}N_5O_4$ $[M+H]^+$: 514.2454; found: 514.2451.

*1-(4-(3-Aminopiperidin-1-yl)-3-(trifluoromethyl)phenyl)-3-(3-(6,7-dimethoxyquinolin-4-yloxy)phenyl)urea hydrochloride (**42b**)* (off-white solid, 56% yield). ^{1}H NMR (400 MHz, DMSO-d_6) δ 9.15 (s, 2H), 8.51 (d, J = 5.0 Hz, 1H), 7.87 (s, 1H), 7.57 (s, 2H), 7.52 (s, 1H), 7.41 (d, J = 6.8 Hz, 3H), 7.30 (d, J = 7.7 Hz, 1H), 6.89 (d, J = 7.5 Hz, 1H), 6.56 (d, J = 4.9 Hz, 1H), 3.95 (s, 6H), 2.91 (d, J = 8.5 Hz, 2H), 2.86 – 2.68 (m, 4H), 2.58 (d, J = 10.0 Hz, 1H), 2.37 (t, J = 9.1 Hz, 1H), 1.81 (d, J = 7.8 Hz, 1H), 1.70 (d, J = 10.8 Hz, 1H), 1.54 (d, J = 9.8 Hz, 1H). ^{13}C NMR (101 MHz, DMSO-d_6) δ 159.91, 155.01, 153.02, 149.87, 149.30, 147.11, 142.01, 137.06, 130.91, 125.71, 123.45, 115.73, 114.45, 110.83, 108.35, 104.15 99.54, 62.68, 56.15, 54.64, 48.62, 33.44 (s, 1H). LC-MS (ESI, m/z): calcd for $C_{30}H_{31}F_3N_5O_4$ $[M+H]^+$: 582.2328; found: 582.2319.

*1-(4-(4-(Aminomethyl)piperidin-1-yl)-3-(trifluoromethyl)phenyl)-3-(3-(6,7-dimethoxyquinolin-4-yloxy)phenyl)urea hydrochloride (**42c**)* (off -white solid, 45% yield). ^{1}H NMR (400 MHz, DMSO-d_6) δ 9.40 (s, 2H), 8.50 (d, J = 4.2 Hz, 1H), 7.87 (s, 1H), 7.57 (s, 2H), 7.51 (s, 1H), 7.41 (s, 3H), 7.31 (d, J = 7.0 Hz, 1H), 6.87 (d, J = 7.0 Hz, 1H), 6.55 (d, J = 4.1 Hz, 1H), 3.95 (d, J = 5.7 Hz, 6H), 3.42 (s, 1H), 2.86 (d, J = 8.2 Hz, 2H), 2.64 (t, J = 10.3 Hz, 2H), 2.53 (s, 1H), 1.73 (d, J = 10.6 Hz, 2H), 1.36 (s, 1H), 1.21 (d, J = 9.3 Hz, 2H). ^{13}C NMR (101 MHz, DMSO-d_6) δ 159.96 (s, 1H), 154.96, 153.08, 149.87 149.29, 147.51, 146.98, 142.17, 137.11, 130.86, 125.48, 123.40, 116.73, 115.75, 114.36, 110.85, 108.30, 104.13, 99.55, 56.15,

54.27, 47.62, 38.25, 30.70 LC-MS (ESI, m/z): calcd for $C_{31}H_{33}F_3N_5O_4$ $[M+H]^+$: 596.2485; found: 596.2488.

1-(4-(4-Aminopiperidin-1-yl)-3-(trifluoromethyl)phenyl)-3-(3-(6,7-dimethoxyquinolin-4-yloxy)phenyl)urea hydrochloride ***(42d)*** (light yellow solid) ^{1}H NMR (400 MHz, DMSO-d_6) δ 10.18 (s, 1H), 10.09 (s, 1H), 8.80 (d, J = 6.4 Hz, 1H), 8.31 (s, 2H), 7.88 (s, 1H), 7.81 – 7.63 (m, 3H), 7.53 (dd, J = 23.3, 8.0 Hz, 3H), 7.37 (d, J = 8.0 Hz, 1H), 7.02 (d, J = 7.8 Hz, 1H), 6.88 (d, J = 6.5 Hz, 1H), 4.04 (d, J = 3.6 Hz, 6H), 3.12 – 3.02 (m, 1H), 2.92 – 2.89 (m, 2H), 2.80 – 2.75(m, 2H), 2.01 – 1.98 (m, 2H), 1.69 – 1.64 (m, 2H). ^{13}C NMR (101 MHz, DMSO-d_6) δ 156.46, 153.15, 143.02, 142.58, 137.44, 131.48, 126.05, 122.75, 115.81, 114.46, 110.54, 103.67, 100.79, 100.02, 56.95, 52.09, 47.81, 45.74, 30.74. LC-MS (ESI, m/z): calcd for $C_{30}H_{31}F_3N_5O_4$ $[M+H]^+$: 582.2328; found: 582.2331.

tert-Butyl 1-(4-nitro-2-(trifluoromethyl)phenyl)piperidin-4-ylcarbamate ***(43)*** To a solution of **38b** (2.0 g, 8.86 mmol) and K_2CO_3 (3.67 g, 26.58 mmol) in DMF (60 mL) was added **39b** (1.77 g, 8.86 mmol). The mixture was stirred at 100 °C for 8 h, and then the solvent was removed under vacuum after it was allowed to cool down to room temperature. The residue was dissolved in ethyl acetate, washed with water and brine, dried with $MgSO_4$, and then concentrated under vacuum to afford the crude product **43** as a light yellow solid (2.7 g, 79%), which was used in the next step without further purification. LC-MS (ESI, m/z): calcd for $C_{17}H_{23}F_3N_3O_4$ $[M+H]^+$: 390.1641; found: 390.1633.

1-(4-Nitro-2-(trifluoromethyl)phenyl)piperidin-4-amine hydrochloride ***(44)*** Compound **43** (400 mg, 0.637 mmol) was dissolved in 4 M HCl in ethyl acetate (5 mL) at room temperature. The resulting mixture was stirred for 1 h, and then concentrated to afford the product **44** as an off white solid (455 mg), which used in the next step with no further purification. ^{1}H NMR (400

MHz, DMSO-d_6) δ 8.63 – 8.29 (m, 5H), 7.57 (d, J = 8.7 Hz, 1H), 3.32 (d, J = 10.8 Hz, 2H), 3.22 (s, 1H), 2.99 (t, J = 11.2 Hz, 2H), 2.08 (d, J = 10.6 Hz, 2H), 1.73 (d, J = 11.0 Hz, 2H). ^{13}C NMR (101 MHz, DMSO-d_6) δ 157.14, 142.06, 128.92, 124.27, 51.15, 47.39, 30.13 (s, 5H). LC-MS (ESI, m/z): calcd for $C_{12}H_{15}F_3N_3O_2$ $[M+H]^+$: 290.1116; found: 290.1109.

*1-(3-(6,7-Dimethoxyquinolin-4-yloxy)phenyl)-3-(1-(4-nitro-2-(trifluoromethyl)phenyl)piperidin-4-yl)urea (**45**)* To a solution of triphosgene (133 mg, 0.448 mmol) in anhydrous DCM (20 mL) was added a solution of **37** (365 mg, 1.12 mmol), Et_3N (0.2 mL, 1.46 mmol) and DMAP (12 mg, 0.09 mmol) in anhydrous DCM (10 mL) at 0 °C under argon. After stirring for 0.5 h, a solution of **44** (332 mg, 1.12 mmol), Et_3N (0.2mL, 1.46mmol,) and DMAP (12 mg, 0.09 mmol) in anhydrous DCM (10 mL) were added to the above reaction mixture at 0 °C under argon. Then the mixture was warmed to room temperature and stirred for 1 h. The reaction mixture was concentrated and the residue was purified by silica gel flash chromatography with dichloromethane/methanol (20:1) to afford the title compound **45** as an off-white solid (480 mg, 70% yield). ^{1}H NMR (400 MHz, DMSO-d_6) δ 8.61 (s, 1H), 8.51 (s, 1H), 8.39 (s, 2H), 7.52 (dd, J = 30.8, 10.3 Hz, 4H), 7.38 (dd, J = 16.4, 8.4 Hz, 2H), 7.18 (d, J = 8.0 Hz, 1H), 6.81 (d, J = 7.7 Hz, 1H), 6.55 (s, 1H), 6.38 (d, J = 6.4 Hz, 1H), 3.95 (d, J = 7.5 Hz, 6H), 3.69 (s, 1H), 3.29 (d, J = 11.6 Hz, 2H), 3.03 (t, J = 10.9 Hz, 2H), 2.06 – 1.88 (m, 2H), 1.55 (d, J = 11.1 Hz, 2H). LC-MS (ESI, m/z): calcd for $C_{30}H_{29}F_3N_5O_6$ $[M+H]^+$: 612.2070; found: 612.2097.

*1-(1-(4-Amino-2-(trifluoromethyl)phenyl)piperidin-4-yl)-3-(3-(6,7-dimethoxyquinolin-4-yloxy)phenyl)urea (**46**)* To a solution of the compound **45** (480 mg, 0.78 mmol) in methanol (20 mL) was added 10% Pd/C (96 mg, 20% w/w) at room temperature. The reaction mixture was stirred under hydrogen balloon for 8 h, and then filtered through Celite. The filtrate was

concentrated to give the residue which was purified by silica gel flash chromatography with dichloromethane/methanol (20:1) to afford compound **46** as an off white solid (185 mg, 41% yield). ^{1}H NMR (400 MHz, DMSO-d_6) δ 8.57 (s, 1H), 8.50 (s, 1H), 7.50 (s, 2H), 7.37 (dd, J = 17.7, 9.4 Hz, 2H), 7.24 (d, J = 8.1 Hz, 1H), 7.17 (d, J = 7.6 Hz, 1H), 6.88 – 6.71 (m, 3H), 6.54 (s, 1H), 6.30 (s, 1H), 5.33 (s, 2H), 3.95 (d, J = 7.8 Hz, 6H), 3.51 (s, 1H), 2.72 (dd, J = 21.5, 11.5 Hz, 4H), 1.84 (d, J = 9.9 Hz, 2H), 1.49 (d, J = 10.1 Hz, 2H). LC-MS (ESI, m/z): calcd for $C_{30}H_{31}F_3N_5O_4$ $[M+H]^+$: 582.2328; found: 582.2350.

*Methyl 1-((3-((6,7-dimethoxyquinolin-4-yl)oxy)phenyl)carbamoyl)cyclopropane -1- carboxylate (**47**)* To a solution of **37** (200 mg, 0.675 mmol) in DMF (5 mL) was added 1-(methoxycarbonyl)cyclopropane-1-carboxylic acid (116 mg, 0.809 mmol), HATU (333 mg, 0.878 mmol) and DIPEA (0.35 mL, 2.025 mmol). The reaction mixture was allowed to stirr at room temperature overnight. The solvent was removed under vacuum to give the residue which was diluted with ethyl acetate and washed with brine. The organic phase was collected and dried over $MgSO_4$, then filtered through Celite and concentrated. The residue was purified by silica gel flash chromatography with dichloromethane/methanol (20:1) to afford compound **47** as an off white solid (271 mg, 95% yield). ^{1}H NMR (400 MHz, $CDCl_3$) δ 8.50 (d, J = 4.6 Hz, 1H), 7.68 (s, 1H), 7.56 (s, 1H), 7.42 (d, J = 12.5 Hz, 3H), 6.95 (d, J = 0.9 Hz, 1H), 6.54 (d, J = 4.4 Hz, 1H), 4.06 (s, 6H), 3.74 (s, 3H), 1.81 (s, 2H), 1.70 (s, 2H). LC-MS (ESI, m/z): calcd for $C_{23}H_{23}N_2O_6$ $[M+H]^+$: 423.1556; found: 423.1561.

*tert-Butyl (1-(4-(1-((3-((6,7-Dimethoxyquinolin-4-yl)oxy)phenyl)carbamoyl) cyclopropane-1-carboxamido)-2-(trifluoromethyl)phenyl)piperidin-4-yl)carbamate (**48**)* To a solution of **47** (270 mg, 0.639 mmol) in MeOH (10 mL) was added 1.0 M NaOH (aq, 1 mL). The mixture was stirred under reflux for about 2 h. After being cooled down to room temperature, the

reaction mixture was concentrated under vacuum to give the crude product **48**, which was used in the next step without further purification. LC-MS (ESI, m/z): calcd for $C_{22}H_{21}N_2O_6$ $[M+H]^+$: 409.1400; found: 409.1411. To a solution of **48** (130 mg, 0.318 mmol), **40d** (114 mg, 0.318 mmol) and DIPEA (0.11 mL, 0.636 mmol) in DMF (3 mL) was added HATU (183 mg, 0.477 mmol) at room temperature and the reaction mixture was stirred overnight. The solvent was removed under vacuum to give the residue that was diluted with ethyl acetate and washed with water and brine. The organic phase was collected and dried with $MgSO_4$, then filtered and concentrated to give the crude product which was purified by silica gel flash chromatography with dichloromethane/methanol (20:1) to afford the title compound **49** as an off white solid (150 mg, 63% yield). ^{1}H NMR (400 MHz, $CDCl_3$) δ 9.34 (s, 1H), 9.05 (s, 1H), 8.51 (s, 1H), 7.75 (s, 1H), 7.68 (d, *J* = 9.4 Hz, 1H), 7.60 (d, *J* = 1.7 Hz, 1H), 7.56 (s, 1H), 7.45 (s, 2H), 7.37 (s, 1H), 7.31 (d, *J* = 15.0 Hz, 2H), 6.99 (d, *J* = 14.6 Hz, 1H), 6.55 (d, *J* = 5.9 Hz, 1H), 4.06 (s, 6H), 3.65 – 3.55 (m, 1H), 3.05 – 2.97 (m, 2H), 2.83 – 2.75 (m, 2H), 2.06 – 2.02 (m, 2H), 1.98 – 1.92 (m, 2H), 1.73 – 1.69 (m, 2H), 1.63 – 1.58 (m, 2H), 1.48 (s, 9H). LC-MS (ESI, m/z): calcd for $C_{39}H_{43}F_3N_5O_7$ $[M+H]^+$: 750.3115; found: 750.3119.

*N-(4-(4-Aminopiperidin-1-yl)-3-(trifluoromethyl)phenyl)-N-(3-((6,7-dimethoxyquinolin-4-yl)oxy)phenyl)cyclopropane-1,1-dicarboxamide (**50**)* The compound **49** (400 mg, 0.637 mmol,) was dissolved in 4 M HCl in ethyl acetate (5 mL) at room temperature. The resulting mixture was stirred for 1 h, and then concentrated to afford the product **50** as an off white solid (151 mg, 99 %) which was used directly in the next step. LC-MS (ESI, m/z): calcd for $C_{34}H_{35}F_3N_5O_5$ $[M+H]^+$: 650.2590; found: 650.2593.

Cell Lines, Antibodies and Chemicals. The human GIST-T1 cell line was purchased from Cosmo Bio Co., Ltd. (Tokyo, Japan). GIST-5R cell line was kindly provided by Prof. Brian

Rubin, Department of Molecular Genetics, Lerner Research Institute and Department of Anatomic Pathology and Taussing Cancer Center, Cleveland Clinic, Cleveland, OH 44195. GIST-T1 and GIST-5R cell lines were maintained in DMEM (Corning, USA) supplemented with 10% FBS, 1% penicillin/streptomycin. Isogenic BaF3 cells lines were cultured in RPMI 1640 media (Corning, USA) with 10% fetal bovine serum (FBS) and supplemented with 2% L-glutamine and 1% penicillin/ streptomycin. All cell lines were maintained in culture media at 37 °C with 5% CO_2.

The following antibodies were purchased from Cell Signaling Technology (Danvers, MA): AKT (pan) (C67E7) Rabbit mAb (#4691), Phospho-AKT (Thr308) (244F9) Rabbit mAb (#4056), Phospho-AKT (Ser473) (D9E) XP® Rabbit mAb (#4060), GAPDH (D16H11) XP® Rabbit mAb, PARP (46D11) Rabbit mAb (#9532), Caspase-3 (8G10) Rabbit mAb (#9665), Phospho-p44/42 MAPK (ERK1/2) (Thr202/Tyr204) (197G2) Rabbit mAb (#4377), p44/42 MAPK (ERK1/2) (137F5) Rabbit mAb (#4695), cKIT (Ab81) Mouse mAb(#3308), Phospho-cKIT (Tyr703) (D12E12) Rabbit mAb (#3073), Phospho-cKIT (Tyr719) antibody (#3391), Rabbit (polyclonal) anti-cKIT (pY 823) Phospho specific antibody, Phospho-STAT3 (Tyr705) (D3A7) XP Rabbit mAb (Biotinylated) (#4093), STAT3 (D3Z2G) Rabbit mAb #12640, Phospho-S6 Ribosomal protein (Ser235/236) antibody (#2211), S6 Ribosomal protein (5G10) Rabbit mAb #2217.

Imatinib and Sunitinib and were purchased from Shanghai Haoyuan Chemexpress Inc. (Shanghai, China)

General Procedure for Anti-Proliferation Assays. Cells were grown in 96-well culture plates (3000/well). The compounds of various concentrations were added into the plates. Cell proliferation was determined after treatment with compounds for 72 h. Cell viability was

measured using the CellTiter-Glo assay (Promega, USA) according to the manufacturer's instructions, and luminescence was measured in a multilabel reader (Envision, PerkinElmer, USA). Data were normalized to control groups (DMSO) and represented by the mean of three independent measurements with standard error of < 20%. GI_{50} values were calculated using Prism 5.0 (GraphPad Software, San Diego, CA).

TEL-Isogenic Cell Generation. Retroviral constructs for BaF3-cKIT mutants were made based on the pMSCVpuro (Clontech) backbone. For TEL-cKIT vector, the first 1 kb of human TEL gene with an artificial myristoylation sequence (MGCGCSSHPEDD) was cloned into the pMSCVpuro retroviral vector, followed by a 3xFLAG tag sequence and a stop codon. Then, the kinase domain coding sequence of cKIT was inserted in-frame between TEL and 3xFLAG sequences. For full-length expression vectors, the coding sequences of cKIT variants were directly cloned in pMSCVpuro vector with a 3xFLAG tag at the C-terminal end. All mutagenesis were performed using the QuikChange Site-Directed Mutagenesis Kit (Stratagene) following the manufacturer's instructions. Retrovirus was packaged in HEK293T cells by transfecting cKIT-containing MSCV vectors together with two helper plasmids. Virus supernatants were harvested 48 h after transfection and filtered before infection. Then BaF3 cells were infected with harvested virus supernatants using spinoculation protocol and stable cell lines were obtained by puromycin selection for 48 h. The IL-3 concentrations in the culture medium were gradually withdrawn until cells were able to grow in the absence of IL-3.

cKIT Protein Purification. The sequences encoding wt cKIT and T670I cKIT residues 544-935 with a Histag were cloned into baculovirus expression vector pFASTHTA. The proteins were expressed by infecting SF9 cells with high titer viral stocks for 48h. Cells were harvested and lysed in 25 mM Tris pH7.4, 250 mM NaCl, 1 mM PMSF. The supernatant was loaded to Ni-

NTA column (QIAGEN, 1018244). Then the proteins were step-eluted with the same buffer with 250 mM imidazole. The eluted proteins were loaded on a Superdex-200 column equilibrated in 25 mM Tris (pH 7.4), 250 mM NaCl, 1 mM DTT, and 1 mM EDTA. Peak fractions were concentrated to 2 mg/mL and flash-frozen.

Kinase Biochemical Assay. The ADP-Glo kinase assay (Promega, Madison, WI) was used to screen compound **35** for its cKIT, cKIT T670I inhibition effects. The kinase reaction system contains 9 μL cKIT (40 ng/μL) or cKIT T670I (20 ng/μL), 1 μL of serially diluted compound **35**, and 10 μL substrate Poly(4:1 Glu, Tyr) peptide (0.4 μg/μL) (Promega, Madison, WI) with 100 μM ATP (Promega, Madison, WI). The reaction in each tube was started immediately by adding ATP and kept going for 1 h under 37 °C. After the tube was cooled for 5 min at room temperature, 5 μL solvent reactions were carried out in a 384-well plate. Then 5 μL of ADP-Glo reagent was added into each well to stop the reaction and consume the remaining ATP within 40 min. At the end, 10 μL of kinase detection reagent was added into the well and incubated for 30 min to produce a luminescence signal. The luminescence signal was measured with an automated plate reader (Envision, PE, USA), and the dose−response curve was fitted using Prism 5.0 (GraphPad Software Inc., San Diego, CA).

Signaling Pathway Study. GIST-T1 and GIST-5R cells were cultured in 10% FBS-containing DMEM medium. The serially diluted compound **35** was added to cells for 1 h. The cells were collected and lysed. The cell lysates were analyzed by western blotting. Western blotting was performed by standard methods, as previously described.[20]

Apoptosis Effect Examination. GIST-T1 and GIST-5R cells were cultured in 10% FBS-containing DMEM medium. The serially diluted compound **35** was added to cells for 24 h. Then,

apoptosis of GIST-T1 and GIST-5R cells were detected by western-blot using PARP and GAPDH antibodies (Cell Signaling Technology).

In Vivo Pharmacokinetics Study. Compound **35** was dissolved in 55% saline containing 5% DMSO and 40% PEG400 by vortex. The final concentration of the stock solution was 1 mg/mL for administration. Six 8 week old male Sprague-Dawely rats were fasted overnight before starting drug treatment via intravenous and oral administration. Animal blood collection time points were as follows: for group 1, 3, 5 (intravenous): 1 min, 5 min, 15 min, 30 min, 1 h, 2 h, 4 h, 6 h, 8 h before and after administration was selected; for group 2, 4, 6 (oral): 5 min, 15 min, 30 min, 1 h, 2 h, 4 h, 6 h, 8 h and 24 h before and after dosing. Each time about 0.2 mL blood was collected through the jugular vein adding heparin for anticoagulation and kept on ice. Then plasma was separated by centrifugation at 8000 rpm for 6 minutes at 2-8 °C. The obtained plasma was stored at -80 °C before analysis. After finishing the test, all surviving animals will be transferred to the repository or euthanasia (CO_2 asphyxiation).

BaF3-TEL-cKIT-T670I Xenograft Model. Five week old female nu/nu mice were purchased from the Shanghai Experimental Center, Chinese Academy of Sciences (Shanghai, China). All animals were maintained in a specific pathogen-free facility and used according to the animal care regulations of Hefei Institutes of Physical Science, Chinese Academy of Sciences (Hefei, China), and all efforts were made to minimize animal suffering. To obtain orthotopic xenograft of human mammary tumor in the mice, cells were harvested during exponential growth. One million BaF3-TEL-cKIT-T670I cells in PBS were suspended in a 1:1 mixture with Matrigel (BD Biosciences) and injected into the subcutaneous space on the right flank of nu/nu mice. Daily IP injection was initiated when BaF3-TEL-cKIT-T670I tumors had reached a size of 200 to 400 mm3. Animals were then randomized into treatment groups of 7 mice each for

efficacy studies. Compound **35** was delivered daily in a HKI solution (0.5% Methocellulose/0.4% Tween80 in ddH_2O) by IP injection. A range of doses of **35** or its vehicle was administered, as indicated in Figure 9 legend. Body weight and tumor growth were measured daily after **35** treatment. Tumor volumes were calculated as follows: tumor volume (mm3) = [(W2 × L)/2] in which width (W) is defined as the smaller of the two measurements, and length (L) is defined as the larger of the two measurements.

HE Staining. HE staining was carried out according to the previous report.[21] First, the sections were hydrated and then the slide was dipped into a Coplin jar containing Mayer's hematoxylin and agitated for 30 s. After rinsing the slide in H_2O for 1 min, it was stained with 1% eosin Y solution for 10−30 s with agitation. Subsequently, the sections were dehydrated with two changes of 95% alcohol and two changes of 100% alcohol for 30 s each, and then the alcohol was extracted with two changes of xylene. Finally, one or two drops of mounting medium was added and covered with a coverslip.

***K*$_i$-67 Staining.** For IHC demonstration of K_i-67, tissue sections were quenched for endogenous peroxides and placed in an antigen retrieval solution (0.01 M citrate buffer, PH 6.0) for 15 min in a microwave oven at 100 °C at 600W. After incubation in the casein block, mouse mAb anti-K_i-67 (ZSGB-BIO, China) was applied to the sections at dilutions of 1:50. Incubations with primary antibodies lasted overnight at 4 °C. The secondary detection system was used to visualize antibody binding. Staining was developed with DAB, and the slides were counterstained with hematoxylin, dehydrated, and mounted.

TUNEL Staining. TUNEL staining was performed using the POD in Situ Cell Death Detection kit (Roche, USA). Briefly, sections were deparaffinized in xylene, rehydrated in decreasing concentration of ethanol, and then treated by nuclease free Proteinase K for 15 min at

room temperature before endogenous peroxidase was blocked in 3% H_2O_2 in methanol. Terminal deoxynucleotidyl transferase (TdT) in reaction buffer was applied to sections for 1 h at 37 °C. Following washes, the slides were covered by converter-POD solution for 30 min at 37 °C. Apoptotic cells were detected after incubation in 3,3'-diaminobenzidine (DAB) chromogen (Beyotime Biotechnology, China) for approximately 8 min, and the slides were counterstained with hematoxylin.

Molecular Modeling.

The crystal structure of cKIT/imatinib complex (PDB ID: 1T46) was used for docking. Alternative coordinates of the side chains were manually confirmed. Missing side chains were automatically added using AmberTools15.[22] The protonation and tautomeric state at physiological pH were confirmed by software Reduce,[23] and the receptor side-chain coordinates were further optimized by Yeti^X 8.3.[24] The cKIT(T670I) mutant coordinates were generated by first replacing Thr670 with Alanine, then changing the residue name to ILE and automatically adding the missing coordinates by AmberTools15 based on the local environment. The coordinates of compounds **1** and **35** were generated and pre-optimized by Bio^X 4.6[25] and the atomic AM1-BCC partial charges were calculated by antechamber within AmberTools15. Template-based induced-fit docking for the two compounds with both cKIT and cKIT(T670I) were performed by Yeti^X 8.3.

NOTES

Dr. Shanchun Zhang is a shareholder of Hefei Cosource Medicine Technology Co. LTD.

ACKNOWLEDGMENTS

Q.L. is supported by the Joint Funds of Research on Major Science Facilities, Key Program of the National NSFC (#U1432250). W.W., J.L. and Q.L. are supported by the grant of "Cross-disciplinary Collaborative Teams Program for Science, Technology and Innovation (2014-2016)" from Chinese Academy of Sciences. We are grateful for the China "Thousand Talents Program" support for Q.L. and "Hundred Talents Program" of the Chinese Academy of Sciences support for J.L., and W.W. J.L. is also supported by the National Program for Support of Top-notch Young Professionals. Q.L. is also supported by the CAS/SAFEA international partnership program for creative research teams.

ABBREVIATIONS USED

GISTs, gastrointestinal stromal tumors; KIT kinase, v-kit Hardy−Zuckerman 4 feline sarcoma viral oncogene homologue; RTK, receptor tyrosine kinase; SAR, structure−activity relationship; DMSO, dimethylsulfoxide; *t*BuOK, potassium *tert*-butoxide; DMF, *N,N*-dimethylformamide; DCM; dimethylchloride; HATU, 1-[bis(dimethylamino)methylene]-1*H*-1,2,3-triazolo[4,5-b]pyridinium 3-oxid hexafluorophosphate; GI_{50}, half growth inhibition concentration; HE stain, hematoxylin and eosin stain; TUNEL stain, terminal deoxynucleotidyl transferase dUTP nick end labeling stain; DMEM, Dulbecco's modified eagle medium; pMSCV, plasmid murine stem cell virus.

ASSOCIATED CONTENT

Supporting Information

The supporting information is available free of charge on the ACS Publication website at http://pubs.acs.org.

Table S1 listing the DiscoverX's KinomeScan selectivity profiling data of compound **35** (see attached excel file).

AUTHOR INFORMATION

Corresponding Authors

*Phone: 86-551-65593186. E-mail: jingliu@hmfl.ac.cn.

*Phone: 86-551-65595161. E-mail: qsliu97@hmfl.ac.cn.

AUTHOR CONTRIBUTIONS

The manuscript was written through contributions of all authors. All authors have given approval to the final version of the manuscript. B.L., A.W., J.L., Z.Q. and X.L. contributed equally to this work.

REFERENCES

(1) Miettinen, M.; Lasota, J. Gastrointestinal stromal tumors--definition, clinical, histological, immunohistochemical, and molecular genetic features and differential diagnosis. *Virchows Arch.* **2001**, *438*, 1-12.

(2) Lennartsson, J.; Ronnstrand, L. Stem cell factor receptor/c-Kit: from basic science to clinical implications. *Physiol. Rev.* **2012**, *92*, 1619-1649.

(3) Linnekin, D. Early signaling pathways activated by c-Kit in hematopoietic cells. *Int. J. Biochem. Cell Biol.* **1999**, *31*, 1053-1074.

(4) Hirota, S.; Isozaki, K.; Moriyama, Y.; Hashimoto, K.; Nishida, T.; Ishiguro, S.; Kawano, K.; Hanada, M.; Kurata, A.; Takeda, M.; Muhammad Tunio, G.; Matsuzawa, Y.; Kanakura, Y.; Shinomura, Y.; Kitamura, Y. Gain-of-function mutations of c-kit in human gastrointestinal

stromal tumors. *Science* **1998**, *279*, 577-580.

(5) Heinrich, M. C.; Corless, C. L.; Duensing, A.; McGreevey, L.; Chen, C. J.; Joseph, N.; Singer, S.; Griffith, D. J.; Haley, A.; Town, A.; Demetri, G. D.; Fletcher, C. D.; Fletcher, J. A. PDGFRA activating mutations in gastrointestinal stromal tumors. *Science* **2003**, *299*, 708-710.

(6) Joensuu, H.; Roberts, P. J.; Sarlomo-Rikala, M.; Andersson, L. C.; Tervahartiala, P.; Tuveson, D.; Silberman, S.; Capdeville, R.; Dimitrijevic, S.; Druker, B.; Demetri, G. D. Effect of the tyrosine kinase inhibitor STI571 in a patient with a metastatic gastrointestinal stromal tumor. *N. Engl. J. Med.* **2001**, *344*, 1052-1056.

(7) Demetri, G. D.; von Mehren, M.; Blanke, C. D.; Van den Abbeele, A. D.; Eisenberg, B.; Roberts, P. J.; Heinrich, M. C.; Tuveson, D. A.; Singer, S.; Janicek, M.; Fletcher, J. A.; Silverman, S. G.; Silberman, S. L.; Capdeville, R.; Kiese, B.; Peng, B.; Dimitrijevic, S.; Druker, B. J.; Corless, C.; Fletcher, C. D.; Joensuu, H. Efficacy and safety of imatinib mesylate in advanced gastrointestinal stromal tumors. *N. Engl. J. Med.* **2002**, *347*, 472-480.

(8) Verweij, J.; Casali, P. G.; Zalcberg, J.; LeCesne, A.; Reichardt, P.; Blay, J. Y.; Issels, R.; van Oosterom, A.; Hogendoorn, P. C.; Van Glabbeke, M.; Bertulli, R.; Judson, I. Progression-free survival in gastrointestinal stromal tumours with high-dose imatinib: randomised trial. *Lancet* **2004**, *364*, 1127-1134.

(9) Antonescu, C. R.; Besmer, P.; Guo, T.; Arkun, K.; Hom, G.; Koryotowski, B.; Leversha, M. A.; Jeffrey, P. D.; Desantis, D.; Singer, S.; Brennan, M. F.; Maki, R. G.; DeMatteo, R. P. Acquired resistance to imatinib in gastrointestinal stromal tumor occurs through secondary gene mutation. *Clin. Cancer Res.* **2005**, *11*, 4182-4190.

(10) Debiec-Rychter, M.; Cools, J.; Dumez, H.; Sciot, R.; Stul, M.; Mentens, N.; Vranckx, H.; Wasag, B.; Prenen, H.; Roesel, J.; Hagemeijer, A.; Van Oosterom, A.; Marynen, P. Mechanisms

of resistance to imatinib mesylate in gastrointestinal stromal tumors and activity of the PKC412 inhibitor against imatinib-resistant mutants. *Gastroenterology* **2005**, *128*, 270-279.

(11) Heinrich, M. C.; Corless, C. L.; Blanke, C. D.; Demetri, G. D.; Joensuu, H.; Roberts, P. J.; Eisenberg, B. L.; von Mehren, M.; Fletcher, C. D.; Sandau, K.; McDougall, K.; Ou, W. B.; Chen, C. J.; Fletcher, J. A. Molecular correlates of imatinib resistance in gastrointestinal stromal tumors. *J. Clin. Oncol.* **2006**, *24*, 4764-4774.

(12) Gajiwala, K. S.; Wu, J. C.; Christensen, J.; Deshmukh, G. D.; Diehl, W.; DiNitto, J. P.; English, J. M.; Greig, M. J.; He, Y. A.; Jacques, S. L.; Lunney, E. A.; McTigue, M.; Molina, D.; Quenzer, T.; Wells, P. A.; Yu, X.; Zhang, Y.; Zou, A.; Emmett, M. R.; Marshall, A. G.; Zhang, H. M.; Demetri, G. D. KIT kinase mutants show unique mechanisms of drug resistance to imatinib and sunitinib in gastrointestinal stromal tumor patients. *Proc. Natl. Acad. Sci. U. S. A.* **2009**, *106*, 1542-1547.

(13) Wardelmann, E.; Merkelbach-Bruse, S.; Pauls, K.; Thomas, N.; Schildhaus, H. U.; Heinicke, T.; Speidel, N.; Pietsch, T.; Buettner, R.; Pink, D.; Reichardt, P.; Hohenberger, P. Polyclonal evolution of multiple secondary KIT mutations in gastrointestinal stromal tumors under treatment with imatinib mesylate. *Clin. Cancer Res.* **2006**, *12*, 1743-1749.

(14) Weisberg, E.; Manley, P. W.; Breitenstein, W.; Bruggen, J.; Cowan-Jacob, S. W.; Ray, A.; Huntly, B.; Fabbro, D.; Fendrich, G.; Hall-Meyers, E.; Kung, A. L.; Mestan, J.; Daley, G. Q.; Callahan, L.; Catley, L.; Cavazza, C.; Azam, M.; Neuberg, D.; Wright, R. D.; Gilliland, D. G.; Griffin, J. D. Characterization of AMN107, a selective inhibitor of native and mutant Bcr-Abl. *Cancer Cell* **2005**, *7*, 129-141.

(15) Adenis, A.; Blay, J. Y.; Bui-Nguyen, B.; Bouche, O.; Bertucci, F.; Isambert, N.; Bompas, E.; Chaigneau, L.; Domont, J.; Ray-Coquard, I.; Blesius, A.; Van Tine, B. A.; Bulusu, V. R.;

Dubreuil, P.; Mansfield, C. D.; Acin, Y.; Moussy, A.; Hermine, O.; Le Cesne, A. Masitinib in advanced gastrointestinal stromal tumor (GIST) after failure of imatinib: a randomized controlled open-label trial. *Ann. Oncol.* **2014**, *25*, 1762-1769.

(16) Guo, T.; Agaram, N. P.; Wong, G. C.; Hom, G.; D'Adamo, D.; Maki, R. G.; Schwartz, G. K.; Veach, D.; Clarkson, B. D.; Singer, S.; DeMatteo, R. P.; Besmer, P.; Antonescu, C. R. Sorafenib inhibits the imatinib-resistant KITT670I gatekeeper mutation in gastrointestinal stromal tumor. *Clin. Cancer Res.* **2007**, *13*, 4874-4881.

(17) Zhao, Z.; Wu, H.; Wang, L.; Liu, Y.; Knapp, S.; Liu, Q.; Gray, N. S. Exploration of type II binding mode: A privileged approach for kinase inhibitor focused drug discovery? *ACS Chem. Biol.* **2014**, *9*, 1230-1241.

(18) Davis, M. I.; Hunt, J. P.; Herrgard, S.; Ciceri, P.; Wodicka, L. M.; Pallares, G.; Hocker, M.; Treiber, D. K.; Zarrinkar, P. P. Comprehensive analysis of kinase inhibitor selectivity. *Nat. Biotechnol.* **2011**, *29*, 1046-1051.

(19) Grunewald, S.; Mühlenberg, T.; Rubin, B.; Schuler, M. H.; Fletcher, J. A.; Bauer, S. Effect of secondary KIT mutations on growth of GIST cells in the absence of selective pressure by imatinib in isogenic models of imatinib resistance. *J. Clin. Oncol.*, **2014**, ASCO Annual Meeting Abstracts. *32*, No 15_suppl (May 20 Supplement), 2014: 10555.

(20) Duensing, A.; Medeiros, F.; McConarty, B.; Joseph, N. E.; Panigrahy, D.; Singer, S.; Fletcher, C. D.; Demetri, G. D.; Fletcher, J. A. Mechanisms of oncogenic KIT signal transduction in primary gastrointestinal stromal tumors (GISTs). *Oncogene* **2004**, *23*, 3999−4006.

(21) Pollard, J. W. Trophic macrophages in development and disease. *Nat. Rev. Immunol.* **2009**, *9*, 259-270.

(22) Case, D. A.; Babin, V.; Berryman, J. T.; Betz, R. M.; Cai, Q.; Cerutti, D. S.; Cheatham, T. A., III; Darden, T. A.; Duke, R. E.; Gohlke, H.; Gietz, A. W.; Gusarov, S.; Homeyer, N.; Jonowski, P.; Kaus, J.; Kolossva·ry, I.; Kovalenko, A.; Lee, T. S.; LeGrand, S.; Luchko, T.; Luo, R.; Madei, B.; Merz, K. M.; Paesani, F.; Roe, D. R.; Roitberg, A.; Sagui, C.; Salomon-Ferrer, R.; Seabra, G.; Simmerling, C. L.; Smith, W.; Swails, J.; Walker, R. C.; Wang, J.; Wolf, R. M.; Wu, X.; Kollman, P. A. AMBER14; University of California: San Francisco, CA, 2014.

(23) Word, J. M.; Lovell, S. C.; Richardson, J. S.; Richardson, D. C. Asparagine and glutamine: using hydrogen atom contacts in the choice of side-chain amide orientation. *J. Mol. Biol*. **1999**, *285*, 1735−1747.

(24) Rossato, G.; Ernst, B.; Smies˘ko, M.; Spreafico, M.; Vedani, A. Probing small-molecule binding to cytochrome P450 2D6 and 2C9: An in silico protocol for generating toxicity alerts. *ChemMedChem* **2010**, *5*, 2088−2101.

(25) Dobler, M. BioX, a versatile molecular-modeling software; Biographics Laboratory 3R: Basel, Switzerland, 2012, http://www.biograf.ch/index.php?id=software (Updated Nov 8, 2014).

Table of Contents Graphic

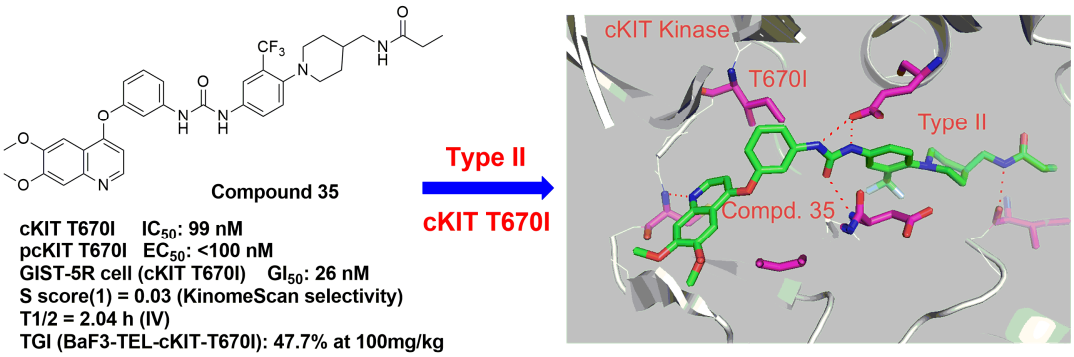

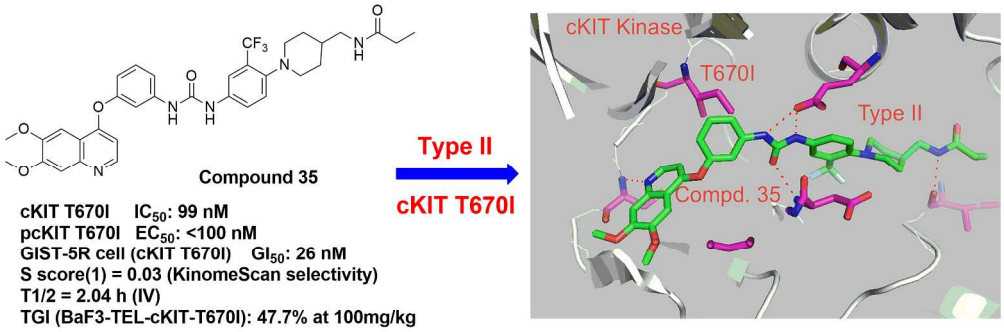

236x78mm (300 x 300 DPI)